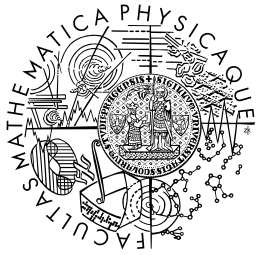

FACULTY
OF MATHEMATICS
AND PHYSICS
Charles University

MASTER THESIS

Bc. Lukáš Vacek

Numerical solution of traffic flow models

Department of Numerical Mathematics

Supervisor of the master thesis:	doc. RNDr. Václav Kučera, Ph.D.
Study programme:	Mathematics (N1101)
Study branch:	MNVM (1101T041)

Prague 2018

I declare that I carried out this master thesis independently, and only with the cited sources, literature and other professional sources.

I understand that my work relates to the rights and obligations under the Act No. 121/2000 Sb., the Copyright Act, as amended, in particular the fact that the Charles University has the right to conclude a license agreement on the use of this work as a school work pursuant to Section 60 subsection 1 of the Copyright Act.

In ..... date ....
signature of the author

Acknowledgments

First, I would like to thank my adviser, Václav Kučera, for all the time and help he gave to me not only for this thesis, but throughout all my years at Charles University. His encouragement and support were more than I could have asked for. He prepared me for the SVOČ competition and helped me with English.

My gratitude also goes to the Faculty of Mathematics and Physics. I enjoyed a master's degree in the Czech Republic. I would like to thank everybody from the Department of Numerical Mathematics. I am very happy that the university gave me the opportunity to study abroad. The semester at the University of Hamburg gave me a lot of experience. I would like to thank Professor Ingenuin Gasser and Hannes von Allwörden. They taught me a lot about traffic flow models.

Most importantly, I thank my parents for raising me in the right way and providing me with the many wonderful opportunities I have had in my life. Their tireless and unending support have been invaluable to me. Last but not least, I thank my brother Michal. I have spent much time with him and always been helpful.

I would like to extend my thanks to all my friends with whom I have met in Teplice, Prague and Hamburg. Special thanks to Honza Nosek who has been studying with me for 14 years, Jára Šedina and Zdeňek Mihula with whom I met at my first lecture at the university and they have been helping me all the time, and Dawit Abiy and Albane Sofia who spent a lot of time with me in Hamburg.

Title: Numerical solution of traffic flow models

Author: Bc. Lukáš Vacek

Department: Department of Numerical Mathematics

Supervisor: doc. RNDr. Václav Kučera, Ph.D., Department of Numerical Mathematics

Abstract: Our work describes the simulation of traffic flows on networks. These are described by partial differential equations. For the numerical solution of our models, we use the discontinuous Galerkin method in space and a multistep method in time. This combination of the two methods on networks is unique and leads to a robust numerical scheme. We use several different approaches to model the traffic flow. Thus, our program must solve both scalar problems as well as systems of equations described by first and second order partial differential equations. The output of our programs is, among other things, the evolution of traffic density in time and 1D space. Since this is a physical quantity, we introduce limiters which keep the density in an admissible interval. Moreover, limiters prevent spurious oscillations in the numerical solution. All the above is performed on networks. Thus, we must deal with the situation at the junctions, which is not standard. The main task is to ensure that the law of conservation of the total amount of cars passing through the junction is still satisfied. This is achieved by modifying the numerical flux for junctions. The result of this work is the comparison of all the models, the demonstration of the benefits of the discontinuous Galerkin method and the influence of limiters.

Keywords: traffic flow, junctions, Discontinuous Galerkin Method (DG), numerical solution

Contents

Introduction

Let us have a road and an arbitrary number of cars. We would like to model the movement of cars on our road. We call this model a traffic flow model. There are two main ways how to describe traffic flow. The first way is the *microscopic model*. Microscopic models describe every car and we can specify the behaviour of every driver and type of car. The basic microscopic models are described by ordinary differential equations (ODEs). The second approach is the *macroscopic model*. In that case, we transform our traffic situation into a continuum and study the density of cars in every point of the road. This model is described by partial differential equations (PDEs). The basic idea was described by James Lighthill and Gerald Whitham in the 1950s. They used conservation laws, because the number of cars is conserved. Specifically, they used Navier-Stokes equations.

Our aim is to study macroscopic models of traffic flow. Our unknown is density at point x and at time t. As we shall see later, the solution can be discontinuous. Due to the need for discontinuous approximation of density, we use the discontinuous Galerkin method. We write the program which calculates the solution. The first version of our program calculates traffic flow on one road. We can test different types of mathematical descriptions of traffic and compare them. Later we extended our program and now we can calculate traffic flow on networks. The aim of modelling is understanding traffic dynamics and deriving possible control mechanisms for traffic.

This work is divided into five chapters. The first four chapters are theoretical. The first three are about *traffic flow*. We define microscopic and macroscopic models, describe our mathematical models for the macroscopic model and solve the problem on junctions. In the fourth chapter we define the *discontinuous Galerkin method* and transform our mathematical model from the third chapter into a finite dimensional numerical model. We will speak about our program, describe its important parts and interpret our test function space. In the last chapter, we present our numerical solutions.

1. Introduction into traffic flow

We begin with the description of vehicular traffic. We summarize the history, define new fundamental quantities and introduce the main modelling approaches. We follow the lecture "Traffic Flow Models" by Ingenuin Gasser from University of Hamburg and the paper by Femke van Wagenigen-Kessels et al. [1] for introducing the traffic flow theory.

In the two following chapters, we describe microscopic and macroscopic models and study some specific cases in the macroscopic models like junctions. We will show the differences between the modelling approaches. Since our aim is the macroscopic models, we don't study other models in such detail.

1.1 History

The study of vehicular traffic has a long tradition. The first important paper on traffic flow, A study of Traffic Capacity by Bruce D. Greenshields [2], was written in 1935. In this paper he described a relation between traffic density and traffic flow. Many traffic flow modelling approaches were proposed in the fifties of the 20th century. A lot of them are still used. Due to the better understanding of non-linear problems, there were developed some new traffic flow modelling approaches in the nineties of the last century.

The motivation for research was two important aspects: ecological and economical. The ecological aspect is based on prevention of traffic jams. This can reduce fuel consumption, air pollution and noise production. The economical one relates to time lost in dense traffic. Everybody knows that "time is money". The second problem in dense traffic is stop and go movement, which increases fuel consumption and means more money spent on fuel.

1.2 Fundamental quantities

The first important question is which quantities are interesting for us. From this reason we come up with three fundamental quantities. The first one is the *traffic flow*.

Definition 1 (Traffic flow)**.** *Let $\Delta N(x,\Delta T)$ be the number of cars which pass a certain position x in the time interval ΔT. Then we define the traffic flow as*

$$Q(x,t) = \lim_{\Delta T \to t} \frac{\Delta N(x,\Delta T)}{\Delta T}, \tag{1.1}$$

where x is a given position and t is a given time. The unit of traffic flow is the number of cars per second.

This quantity can be easily measured from real traffic situations. Equation (1.1) in the previous definition isn't written mathematically precisely. The right--hand side should be rewritten as a derivative of N with respect to time where ΔT is the neighbourhood of the point t and the size of this neighbourhood tends to zero. The problem is that this definition is hard to use for measurement. If

the time interval is too short, we obtain only two options $N = 1$ or $N = 0$. This depends on the presence of a car at the position x in the time t. In practical measurement we take higher ΔT which can represent the actual traffic situation.

Our next quantity is the *traffic density*.

Definition 2 (Traffic density)**.** *Let $\Delta N(\Delta X,t)$ be the number of cars which pass the space interval ΔX in a certain time. Then we define the traffic density as*

$$\rho(x,t) = \lim_{\Delta X \to x} \frac{\Delta N(\Delta X,t)}{\Delta X}, \tag{1.2}$$

where x is a given position and t is a given time. The unit of traffic density is the number of cars per meter.

Again, as in Definition 1, we do not use precisely the right-hand side in equation (1.2). The reason is the same as above.

The last quantity is the *mean traffic flow velocity* and this quantity is defined by the quantities above.

Definition 3 (Mean traffic flow velocity)**.** *Let Q be the traffic flow and let ρ be traffic density. Then we define the mean traffic flow velocity as*

$$V(x,t) = \frac{Q(x,t)}{\rho(x,t)},$$

where x is a given position and t is a given time. The unit of mean traffic flow velocity is meters per second.

We note that this quantity is not the velocity of a single car in general. We can imagine this quantity as a velocity of a "group" of cars in the neighbourhood of the point x. The cars in this "group" could have different velocities. Even the position x without a car could have non-zero mean traffic flow velocity.

1.3 Fundamental diagram

As we mentioned above (Section 1.1), Greenshields described a relation between traffic density and traffic flow in the paper [2]. He realised that traffic flow is a function which depends only on one variable in homogeneous traffic (traffic with no changes in time and space). This one variable is traffic density. This implies that even mean traffic flow velocity depends only on traffic density. Let us denote the equilibrium quantity Q_e derived from Q and the equilibrium quantity V_e derived from V. Then these equilibrium quantities corresponding to homogeneous traffic satisfy:

$$Q_e(\rho) = \rho V_e(\rho) \tag{1.3}$$

and

$$\frac{\mathrm{d}V_e(\rho)}{\mathrm{d}\rho} \leq 0. \tag{1.4}$$

Equation (1.3) is obtained from Definition 3. Inequality (1.4) states that the equilibrium mean traffic flow velocity decreases with increasing traffic density. Thus,

we can reach the maximal equilibrium traffic flow at a certain density value. In most of the models we have a strictly decreasing $V_e(\rho)$. The relationship between the traffic density and the mean traffic flow velocity or traffic flow is described by the *fundamental diagram*. Typical fundamental diagrams are shown in Figure 1.1 and Figure 1.2. The blue line in both figures represent the Greenshields model.

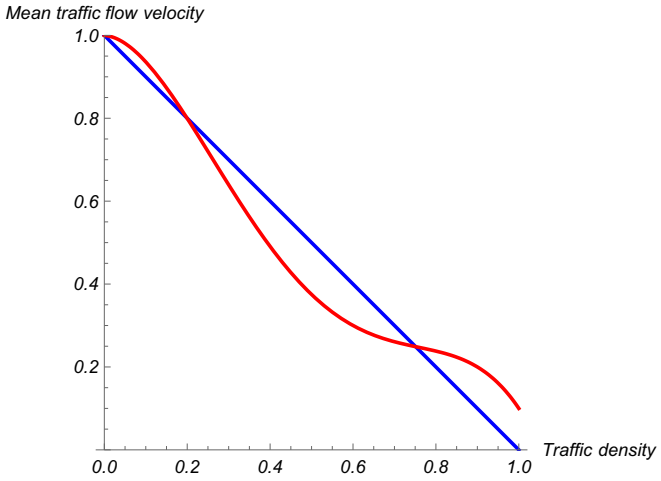

Figure 1.1: Examples of velocity-density diagrams.

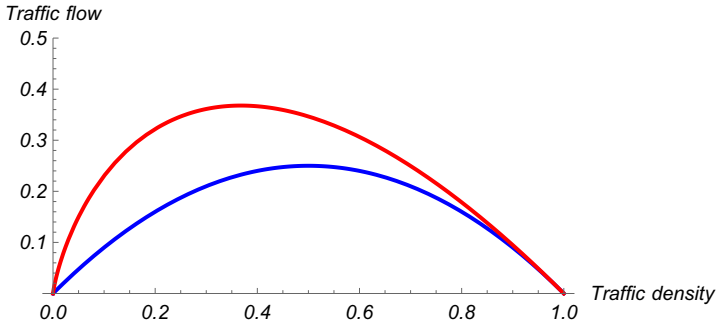

Figure 1.2: Examples of flow-density diagrams.

1.4 Modelling approaches

There are three different modelling approaches: microscopic, kinetic and macroscopic. These approaches are derived from mechanics or fluid dynamics approaches.

In the microscopic approach, we study every car separately. We index cars by $i = 1, \ldots, N$ and represent the car by coordinate $x_i(t) \in \mathbb{R}$ and velocity $v_i(t) \in [0, v_{\max}]$, where $v_{\max}$ is the maximal velocity. Let M be a subset of $\mathbb{R} \times [0, v_{\max}]$, then the number of cars N_M in the subset M is given by:

$$N_M = \sum_{i=1}^{N} \chi_M(x_i, v_i),$$

where χ_M is the characteristic function of the set M. The aim of the microscopic approach is to determine x_i and v_i under certain initial and boundary conditions. Microscopic models are similar to particle models in mechanics.

In the kinetic approach, we use the distribution function $f(x,v,t)$ which describes the density of cars at a point x with a velocity v at a time t. Then the number of cars N_M in the subset M at time t is given by

$$N_M(t) = \int_M f(x,v,t)\ \mathrm{d}x\mathrm{d}v.$$

The aim of the kinetic approach is to find the distribution function f. The idea of the kinetic approach is the same as in the kinetic description in gas dynamics, where f satisfies the Boltzmann equation.

In the macroscopic approach, we use the distribution function f obtained from the kinetic approach to derive macroscopic quantities like *density* ρ, *mean velocity* V and *variance of velocity* Θ:

$$\begin{aligned}
\rho(x,t) &= \int_0^{v_{\max}} f(x,v,t)\ \mathrm{d}v,\\
V(x,t) &= \frac{1}{\rho(x,t)} \int_0^{v_{\max}} v f(x,v,t)\ \mathrm{d}v,\\
\Theta(x,t) &= \frac{1}{\rho(x,t)} \int_0^{v_{\max}} (v - V(x,t))^2 f(x,v,t)\ \mathrm{d}v.
\end{aligned}$$

This transformation from the kinetic to the macroscopic approach is similar to such a transformation in gas dynamics from which, for example, the Euler and the Navier-Stokes equations can be derived. The aim of the macroscopic approach is to find an equation for ρ, V and Θ.

As we mentioned above (Section 1.3), Greenshields realised in the paper [2] that we have some special properties for homogeneous traffic flow. Homogeneous traffic flow is a time and a space independent traffic situation. We already know that the mean traffic flow velocity depends only on the density. Therefore, we have an equilibrium distribution function $f_e(\rho,v)$ in the kinetic approach. In the macroscopic approach we have

$$\begin{aligned}
V_e(\rho) &= \frac{1}{\rho} \int_0^{v_{\max}} v f_e(\rho,v)\ \mathrm{d}v,\\
\Theta_e(\rho) &= \frac{1}{\rho} \int_0^{v_{\max}} (v - V_e(\rho))^2 f_e(\rho,v)\ \mathrm{d}v.
\end{aligned}$$

There are a lot of different models for V_e. For example, the Greenshields model in Figure 1.1 and Figure 1.2 (blue line) uses

$$V_e(\rho) = v_{\max}\left(1 - \frac{\rho}{\rho_{\max}}\right),$$

where $\rho_{\max}$ is the maximal traffic density. To define equilibrium quantities correctly, we introduce some conditions which should be satisfied:

- $V_e(0) = v_{\max}$, i.e. the equilibrium mean velocity tends to the maximal velocity in the case with very low density,
- $V_e(\rho_{\max}) = 0$, i.e. the equilibrium mean velocity tends to zero in the case with very high density,
- $V_e(\rho)$ is (strictly) monotone, i.e. the equilibrium mean velocity is decreasing with higher density.

2. Microscopic models

As we mention at the beginning of Chapter 1, we don't study the microscopic models in detail. The reason, why we introduce the theory of microscopic models, is to present other important models which are used. It is good to understand differences between microscopic and macroscopic models, see the pros and cons of both approaches and decide which approach is better for a particular traffic situation and particular traffic network.

There are many different microscopic models. The most important approaches are "car following models" and cellular automata. We study only typical car following models consisting of a second order ODE for every car. We introduce these two approaches in the following subsections.

We use the notation from Section 1.4, so $x_i(t)$ denotes the position of the i^{th} car at time t. The car in front of the i^{th} car is the car with index $i+1$. It is easy to calculate the velocity and acceleration or deceleration of the i^{th} car by derivatives of x_i:

$$v_i(t) = x_i'(t),$$
$$a_i(t) = x_i''(t).$$

2.1 Car following model

We follow the lecture by Gasser and paper by Wilson and Ward [3] for describing the car following model and studying the stability of a solution.

2.1.1 Bando model

Now we consider a circular road. We have two reasons for this: there exists a real experiment (see [4]) and we can analyse the problem with known methods. Let L be the length of the circular road and N be the number of cars. Then we use model introduce by Masamitsu Bando et al. [5]

$$x_i''(t) = \frac{1}{\tau}\left(V_{\text{opt}}\left(x_{i+1}(t) - x_i(t)\right) - x_i'(t)\right), \quad i = 1,\ldots,N, \quad x_{N+1} = x_1 + L, \quad (2.1)$$

where $V_{\text{opt}}(y)$ denotes the desired optimal velocity for a given headway y (distance to the car in front) and τ denotes the reaction time of a "driver-car" system. The equation (2.1) says that the i^{th} car accelerates or decelerates when its velocity is lower or higher than the optimal velocity. The constant τ determines, how fast we want to reach the optimal velocity. The function $V_{\text{opt}}(y)$ is different from the mean traffic flow velocity denoted by $V(x,t)$ or $V_e(\rho)$, which we introduced in the previous section. We assume that the optimal velocity function V_{opt} is an increasing function from minimal velocity $V_{\text{opt}}(0) = 0$ to maximal velocity $\lim_{y\to\infty} V_{\text{opt}}(y) = v_{\max}$.

In the beginning, we scale the model using

$$\tilde{x}_i = \frac{x_i}{L}, \qquad \tilde{t} = \frac{t}{\tau}, \qquad \tilde{V}_{\text{opt}}(y) = \frac{\tau}{L} V_{\text{opt}}(yL),$$

and obtain the scaled problem

$$\tilde{x}_i''(t) = \tilde{V}_{\text{opt}}\left(\tilde{x}_{i+1}(t) - \tilde{x}_i(t)\right) - \tilde{x}_i'(t), \qquad i = 1,\ldots,N, \qquad \tilde{x}_{N+1} = \tilde{x}_1 + 1. \quad (2.2)$$

Due to the use of scaled problem (2.2), we omit the tildes in the next calculations. It is easy to show, that problem (2.2) has a special solution, which is called a *quasi-stationary solution*, of the form

$$x_i(t) = \frac{1}{N} i + V_{\text{opt}}\left(\frac{1}{N}\right) t, \qquad i = 1,\ldots,N,$$

where all cars drive with constant velocity $V_{\text{opt}}\left(\frac{1}{N}\right)$ and constant headway $\frac{1}{N}$.

Now we introduce new variables

$$y_i(t) = x_{i+1}(t) - x_i(t), \qquad i = 1,\ldots,N, \qquad y_{N+1} = y_1.$$

This variable is a conserved quantity because $\sum_{i=1}^{N} y_i = 1$ holds. Then our problem (2.2) is changed into

$$y_i''(t) = V_{\text{opt}}\left(y_{i+1}(t)\right) - V_{\text{opt}}\left(y_i(t)\right) - y_i'(t), \qquad i = 1,\ldots,N, \qquad y_{N+1} = y_1. \quad (2.3)$$

In the new variables the quasi-stationary solution of the problem (2.3) is given by

$$y_i = \frac{1}{N}, \qquad i = 1,\ldots,N.$$

There is the question of stability of the quasi-stationary solution. We only prepare problem (2.3) into the form which is used in the paper [6] by Gasser and answer the question of stability. All calculations are written in the paper [6]. We linearize function V_{opt} around the quasi-stationary solution (the first order Taylor polynomial for function V_{opt} centred at the point $\frac{1}{N}$). We obtain a new second order ODE

$$y_i''(t) = V_{\text{opt}}'\left(\frac{1}{N}\right)\left(y_{i+1}(t) - y_i(t)\right) - y_i'(t), \qquad i = 1,\ldots,N, \qquad y_{N+1} = y_1. \quad (2.4)$$

Then we rewrite (2.4) as a system of two first order ODEs. Taking $z_i = y_i'$ and $(Y_i,Z_i) = (y_i - 1/N, z_i)$ we obtain

$$\begin{aligned} Y_i' &= Z_i \\ Z_i' &= -Z_i + \beta(Y_{i+1} - Y_i), \end{aligned} \quad (2.5)$$

where we denote $\beta = V_{\text{opt}}'\left(\frac{1}{N}\right) \geq 0$ and $i = 1,\ldots,N$. The quasi-stationary solution is $(Y_i,Z_i) = (0,0)$. We can rewrite (2.5) in matrix form

$$\begin{bmatrix} Y_1' \\ \vdots \\ \vdots \\ Y_N' \\ Z_1' \\ \vdots \\ \vdots \\ Z_N' \end{bmatrix} = \begin{bmatrix} 0 & & & & & 1 & & & \\ & \ddots & & & & & \ddots & & \\ & & \ddots & & & & & \ddots & \\ & & & 0 & & & & & 1 \\ -\beta & \beta & & & & -1 & & & \\ & \ddots & \ddots & & & & \ddots & & \\ & & \ddots & \beta & & & & \ddots & \\ & & & -\beta & & & & & -1 \end{bmatrix} \begin{bmatrix} Y_1 \\ \vdots \\ \vdots \\ Y_N \\ Z_1 \\ \vdots \\ \vdots \\ Z_N \end{bmatrix}. \quad (2.6)$$

The quasi-stationary solution is stable if and only if the real parts of eigenvalues of the matrix in equation (2.6) are negative. Since one of the eigenvalue is equal to 0, we must use the conserved quantity and reduce the dimension of the system. As we mention above, following technical steps are in paper [6] in detail. Finally, the quasi-stationary solution is stable if (notation with tilde is used again)

$$\beta = \tilde{V}'_{\text{opt}}\left(\frac{1}{N}\right) = \tau V'_{\text{opt}}\left(\frac{L}{N}\right) < \frac{1}{1+\cos\frac{2\pi}{N}} \tag{2.7}$$

is satisfied. As we can see, stability is dependent on the reaction time and traffic density (ratio between length of circuit and number of cars). Figure 2.1 show the curve which divides the L-N plane between stable and unstable regions. A very interesting situation is on the curve (i.e. inequality (2.7) is changed into equality). From the Hopf bifurcation analysis (see [6]) we obtain a periodic solution under certain conditions.

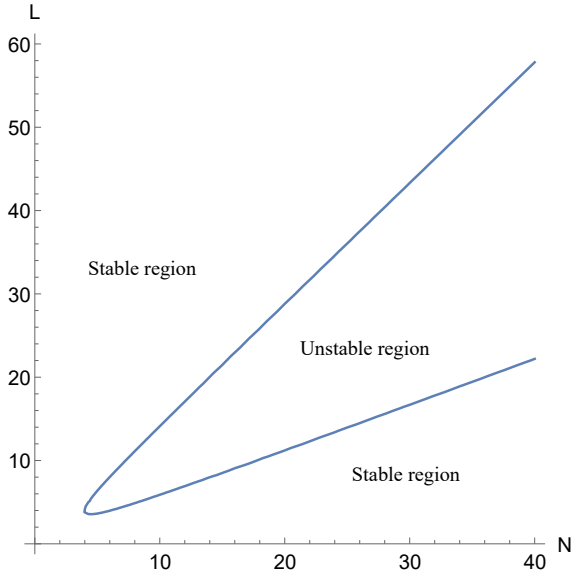

Figure 2.1: The curve dividing stable and unstable regions in the L-N plane.

2.1.2 Other models

Up until now, we study only the Bando model (2.1). Here we introduce other models, which are interesting from the application point of view. Some of them are inspired by the Bando modelling approach. Except the last model, all models are defined for circular roads.

Aggressive drivers model This model is the most interesting approach. Let $\alpha \in [0,1]$ be the degree of non-aggressiveness of the driver. Then we come up with the model

$$\begin{aligned} x''_i(t) = {} & \frac{\alpha}{\tau}\left(V_{\text{opt}}\left(x_{i+1}(t) - x_i(t)\right) - x'_i(t)\right) \\ & + \frac{1-\alpha}{\tau}\left(x'_{i+1}(t) - x'_i(t)\right) F\left(x_{i+1}(t) - x_i(t)\right), \\ i = 1,\ldots,N, \qquad & x_{N+1} = x_1 + L, \end{aligned} \tag{2.8}$$

where $F(y)$ is a function of aggression, which depends on the headway y. The new term in equation (2.8) models the behaviour that the driver accelerates or decelerates more or less aggressively to match the velocity of the car in front of him. We assume that $F : [0,\infty) \to [0,\infty)$ is a decreasing function.

Individual drivers model In this model, every driver has its own reaction time τ_i and own optimal velocity function $V_i(y)$. In case of the Bando model (2.1), we obtain

$$x_i''(t) = \frac{1}{\tau_i}\left(V_i\left(x_{i+1}(t) - x_i(t)\right) - x_i'(t)\right), \quad i = 1,\ldots,N, \quad x_{N+1} = x_1 + L.$$

Model with non-constant reaction times In this model, τ is not constant any more, but it is a function. One of the options is a function depending on the headways. We can use this function in all the models.

Model with time delay This is another approach focused on time. We take into account the situation from the past. One of the models modifies the Bando model (2.1) and considers the headway at an earlier time. Thus, our model is given by

$$x_i''(t) = \frac{1}{\tau}\left(V_{\text{opt}}\left(x_{i+1}(t-T) - x_i(t-T)\right) - x_i'(t)\right), \\ i = 1,\ldots,N, \qquad x_{N+1} = x_1 + L.$$

Model on an infinite lane The last approach is situated on an infinite lane with infinitely many cars. In case of the Bando model (2.1), we obtain

$$x_i''(t) = V_{\text{opt}}\left(x_{i+1}(t) - x_i(t)\right) - x_i'(t), \quad i \in \mathbb{Z}$$

and a special quasi-stationary solution is given by

$$x_i(t) = id + V_{\text{opt}}(d)t, \qquad i \in \mathbb{Z},$$

where d is an average headway.

2.2 Cellular automaton

Disadvantages of the car following model are both solving the ODE for all cars and the fact that each car follows the car in front of it. Cellular automata have no ODE and overtaking can be managed very easily. For describing the theory of cellular automata, we follow the papers [7] and [8].

We can imagine the cellular automaton as a board game (e.g. Formula 1). We have discrete space and time and even physical quantities (like velocity) take on a finite set of discrete values. A cellular automaton consists of a regular uniform lattice (usually finite in extent) with discrete variables occupying the various site. The state is specified by the values of the variables at each site. The variables at each site are updated simultaneously. The update is based on the state at the preceding iteration, and according to given specific "rules".

We begin with single line model. It is defined as a one-dimensional array with L cells of length l with boundary condition. The length l is equal to the average headway in a traffic jam. Next, we have N cars. Each cell can be occupied by at most one car. Traffic density is given by $\rho = \frac{N}{L}$. Each car may have a velocity from the set $\{v \in \mathbb{N}_0;\ v \in [0,v_{\max}]\}$. The velocity corresponds to the number of cells that a car advances in one iteration and $v_{\max} \in \mathbb{N}$ is the maximal number of cells per iteration. The state of the system at a certain iteration is determined by the distribution of cars among the cells and by the velocity of each car. We use the following notation to describe each state:

- $x(i)$ is the position of the i^{th} car,
- $v(i)$ is the velocity of the i^{th} car,
- $g(i)$ is the gap between the i^{th} and $(i+1)^{th}$ car, i.e. $g(i) = x(i+1) - x(i) - 1$.

The motion of a car is determined by the set of updating rules. We use the following set of rules as an example:

1. Acceleration: If $v(i) < v_{\max}$ and $g(i) \geq v(i) + 1$, then $v(i) = v(i) + 1$.
2. Deceleration: If $v(i) > g(i) - 1$, then $v(i) = g(i)$.
3. Motion: The car is moved by $v(i)$ cells.

In Figure 2.2 we used these rules, $v_{\max} = 5\frac{\text{cells}}{\text{iteration}}$ and periodical boundary condition, i.e. we have a circular road. The iteration 0 is the initial condition, $L = 25$, $N = 7$ and we perform 5 iterations. Each car is represented by a specific colour and the numbers represent the velocity of each car. We can see two phenomena there. First of all, we notice that the traffic jam moves backward. This is a phenomenon from the real traffic situation. The second phenomenon is periodicity. From the 3^{rd} iteration we obtain the periodic solution with a period of L iterations (i.e. 25 iterations).

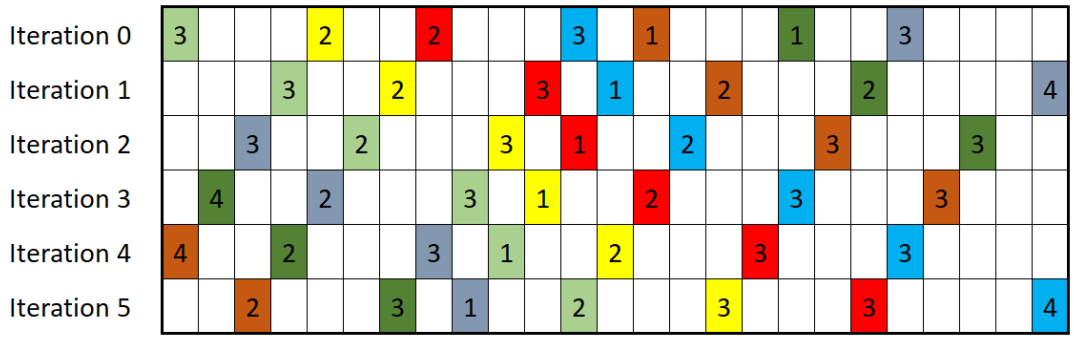

Figure 2.2: Example of the cellular automaton model.

On a multi-line road, we extend the updating rules. At the beginning of each iteration, cars check whether a lane change is suitable or not. Thus, we add a set of lane changing rules. These rules are applied in parallel to each vehicle. We can summarize the rules as follows:

1. The car looks ahead if the existing gap cannot accommodate its current velocity.

2. The car looks sideways if the forward gap on another lane will allow the car to maintain or increase its current velocity.

3. The car looks back if the backward gap on another lane is large enough not to affect the velocity of other cars.

If all the rules are satisfied, then perform a lane change. Once all lane changes are made, the updating rules from the single lane model are applied independently to each line.

3. Macroscopic models

The aim of this chapter is to introduce the modelling of traffic flow using conservation laws. We follow the lecture by Gasser, the lecture notes by Jüngel [9] and the book in progress by Kachroo and Sastry [10].

In the microscopic models we model the cars individually. Now we use density $\rho(x,t)$ of cars in the position $x \in \mathbb{R}$ at the time $t \geq 0$. The number of cars which are in the road section $[x_1,x_2]$ at the time t is

$$\int_{x_1}^{x_2} \rho(x,t) \, \mathrm{d}x.$$

We would like to conserve the number of cars. The difference in the number of cars at the time t_1 and the time t_2 is determined by

$$\int_{x_1}^{x_2} \rho(x,t_2) \, \mathrm{d}x - \int_{x_1}^{x_2} \rho(x,t_1) \, \mathrm{d}x = \int_{x_1}^{x_2} \rho(x,t_2) - \rho(x,t_1) \, \mathrm{d}x. \tag{3.1}$$

Assume that $\rho(x,t)$ is differentiable with respect to time. Then we get

$$(3.1) = \int_{x_1}^{x_2} \int_{t_1}^{t_2} \frac{\partial \rho(x,t)}{\partial t} \, \mathrm{d}t\mathrm{d}x. \tag{3.2}$$

Let $Q(x,t)$ and $V(x,t)$ be the fundamental quantities defined in Section 1.2. The number of cars passing the position x in the time interval $[t_1,t_2]$ is

$$\int_{t_1}^{t_2} Q(x,t) \, \mathrm{d}t.$$

Due to the conservation of the number of cars, we would like to calculate the difference in the number of cars which inflow at the position x_1 and outflow at the position x_2. This difference is given by

$$\int_{t_1}^{t_2} Q(x_1,t) \, \mathrm{d}t - \int_{t_1}^{t_2} Q(x_2,t) \, \mathrm{d}t = \int_{t_1}^{t_2} Q(x_1,t) - Q(x_2,t) \, \mathrm{d}t. \tag{3.3}$$

From Definition 3 we obtain $Q(x,t) = \rho(x,t)V(x,t)$. Assume that $\rho(x,t)$ and $V(x,t)$ are differentiable with respect to position. Then we get

$$(3.3) = -\int_{t_1}^{t_2} \int_{x_1}^{x_2} \frac{\partial \left(\rho(x,t)V(x,t)\right)}{\partial x} \, \mathrm{d}x\mathrm{d}t. \tag{3.4}$$

It will be very helpful if we use the following lemma.

Lemma 1. *Let $\Omega \subset \mathbb{R}^n$ be an open set, $n \in \mathbb{N}$ and $f \in \mathcal{C}(\Omega)$. Then $f \equiv 0$ in Ω if and only if $\int_V f \, \mathrm{d}x = 0$ holds for all open $V \subset \overline{V} \subset \Omega$.*

Proof. We prove both implications:
"$\Rightarrow$": If $f \equiv 0$ then $\int_V f \, \mathrm{d}x = 0$, $\forall V \subset \overline{V} \subset \Omega$.
"$\Leftarrow$": We prove it by contradiction. Let there exists a point $x_0 \in \Omega$ such that $f(x_0) > 0$ without loss of generality. Since f is continuous, there exists neighbourhood of the point x_0, denoted by $U(x_0)$, such that $f(x) > 0$ for all $x \in U(x_0)$.

Then $\int_{U(x_0)} f \mathrm{d}x > 0$ and this is a contradiction with the assumption. □

According to the fact that equation (3.2) and equation (3.4) determine the same difference in the number of cars in the section $[x_1,x_2]$ between the times t_1 and t_2 we can obtain the equality

$$\int_{x_1}^{x_2} \int_{t_1}^{t_2} \frac{\partial \rho(x,t)}{\partial t} \, \mathrm{d}t\mathrm{d}x = - \int_{t_1}^{t_2} \int_{x_1}^{x_2} \frac{\partial \left(\rho(x,t)V(x,t)\right)}{\partial x} \, \mathrm{d}x\mathrm{d}t,$$

i.e.

$$\int_{x_1}^{x_2} \int_{t_1}^{t_2} \frac{\partial}{\partial t}\rho(x,t) + \frac{\partial}{\partial x} \left(\rho(x,t)V(x,t)\right) \, \mathrm{d}t\mathrm{d}x = 0.$$

Since x_1, $x_2 \in \mathbb{R}$ and t_1, $t_2 > 0$ are arbitrary, we can apply Lemma 1 and obtain the PDE

$$\frac{\partial}{\partial t}\rho(x,t) + \frac{\partial}{\partial x} \left(\rho(x,t)V(x,t)\right) = 0, \tag{3.5}$$

where $\rho(x,t)$ and $V(x,t)$ are our unknowns. Equation (3.5) must be supplemented by the initial condition

$$\begin{aligned} \rho(x,0) &= \rho_0(x), \qquad x \in \mathbb{R}, \\ V(x,0) &= V_0(x), \qquad x \in \mathbb{R}. \end{aligned}$$

We have only one equation for two unknowns. Thus, we need an equation for the mean traffic flow velocity $V(x,t)$. There are a lot of approaches. Some of them we introduce later, but now we use the equilibrium velocity $V_e(\rho)$ from Section 1.3. Thus, we have only one unknown $\rho(x,t)$ and equation (3.5) belongs to the class of *non-linear first order hyperbolic equations*.

3.1 Mathematical theory of non-linear first order hyperbolic equations

In this section we study the problem

$$\begin{aligned} u_t + f\left(u\right)_x &= 0, \qquad x \in \mathbb{R},\, t > 0, \\ u(x,0) &= u_0(x), \qquad x \in \mathbb{R}, \end{aligned} \tag{3.6}$$

where $f : \mathbb{R} \to \mathbb{R}$ is a function which is generally non-linear. This problem can be solved by using the *method of characteristics*.

Definition 4 (Characteristics)**.** *Let $u : \mathbb{R} \times [0,\infty) \to \mathbb{R}$ be a (classical) solution of the problem (3.6). Then the solutions $x(t)$ of the initial-value problem*

$$\begin{aligned} x'(t) &= f'\left(u\left(x\left(t\right),t\right)\right), \qquad t > 0, \\ x(0) &= x_0 \end{aligned}$$

are called the characteristics of the problem (3.6).

The main property of the characteristics is that u is constant along them:

$$\begin{aligned} \frac{\mathrm{d}}{\mathrm{d}t}u(x(t),t) &= u_t(x(t),t) + u_x(x(t),t)x'(t) = u_t(x(t),t) + u_x(x(t),t)f'(u(x(t),t)) \\ &= u_t(x(t),t) + f_x(u(x(t),t)) = 0, \qquad t > 0. \end{aligned}$$

We denote $\widehat{u}(t) = u(x(t),t)$. Thus $\widehat{u}(t) = \text{const.}$ for $t > 0$. From the initial condition we obtain

$$\widehat{u}(t) = \widehat{u}(0) = u(x(0),0) = u_0(x_0).$$

Hence, the curves

$$\frac{\mathrm{d}x(t)}{\mathrm{d}t} = f'(\widehat{u}(t)) = f'(u_0(x_0))$$

are straight lines. Thus, the slope of the characteristics depends on the initial condition at the position x_0.

Example. We take $f(u) = u(1-u)$, i.e. $V_e(\rho) = 1-\rho$ in the macroscopic traffic flow. Thus, $f'(u) = 1-2u$. We demonstrate the method of characteristics on different initial conditions.

Example 1 (Figure 3.1): The decreasing initial value u_0 makes no problem. The value $u(x,t)$ is well defined for all $x \in \mathbb{R}$ and $t > 0$ by the characteristics.

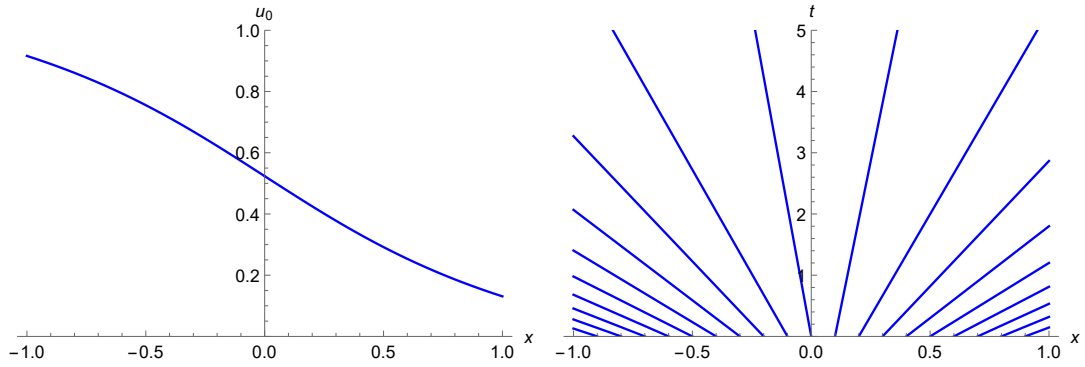

(a) Initial condition. (b) Characteristics.

Figure 3.1: Example 1.

Example 2 (Figure 3.2): Due to the discontinuity of the initial value u_0 at the origin, we obtain a domain without characteristics.

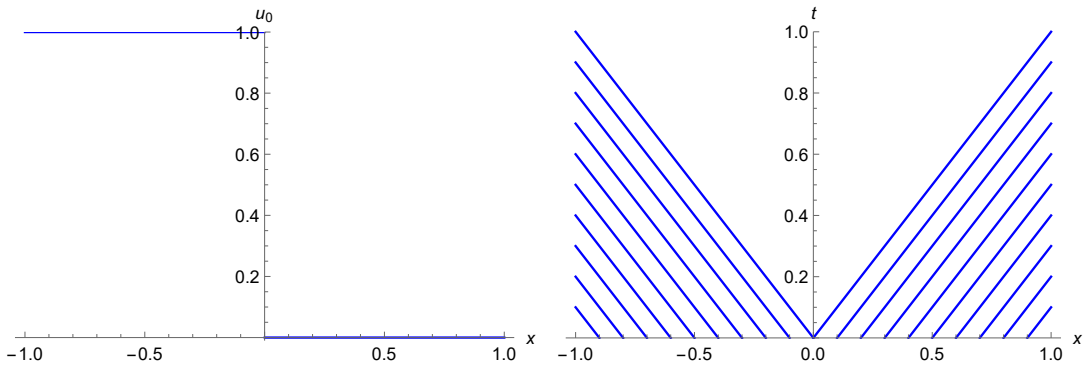

(a) Initial condition. (b) Characteristics.

Figure 3.2: Example 2.

Example 3 (Figure 3.3): Due to the discontinuity of the initial value u_0 at the origin, we obtain more possible values $u(x,t)$ for some $x \in \mathbb{R}$ and $t > 0$ by the characteristic. Thus, we do not obtain a unique solution.

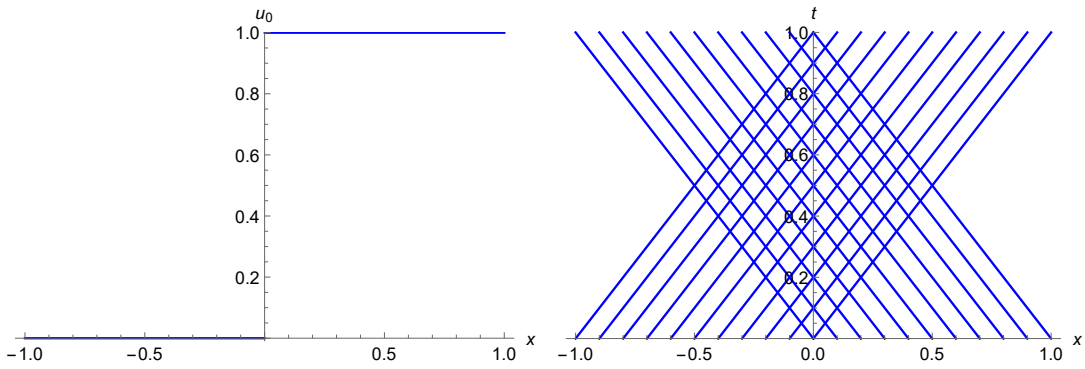

(a) Initial condition. (b) Characteristics.

Figure 3.3: Example 3.

Example 4 (Figure 3.4): The increasing initial value u_0 makes the same problems as Example 3. There exists a time t_0 such that the characteristics intersect each other for $t \geq t_0$. Thus, we do not obtain a unique solution at the time $t \geq t_0$.

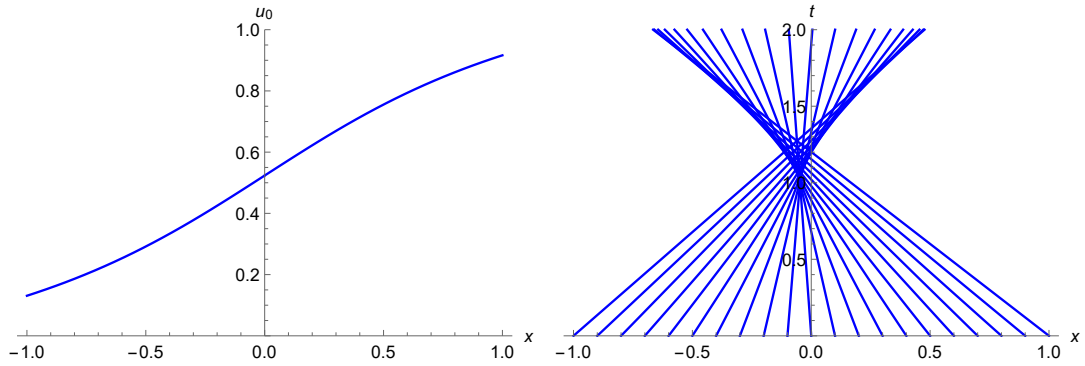

(a) Initial condition. (b) Characteristics.

Figure 3.4: Example 4.

Our examples show us that the method of characteristics can cause some problems. Solutions can be discontinuous and non-unique. Due to the discontinuity, we introduce the *weak formulation* of the problem (3.6) and define the *weak solution*. Later, we obtain the uniqueness from the *entropy conditions*.

The problem (3.6) with initial condition from Figure 3.2a or from Figure 3.3a is known as a *Riemann problem*.

Definition 5 (Riemann problem)**.** *The problem (3.6) with initial datum*

$$u_0(x) = \begin{cases} u_l, & x \leq 0, \\ u_r, & x > 0, \end{cases}$$

where u_l, $u_r \in \mathbb{R}$, is called a Riemann problem.

3.1.1 Weak solution

Let u be a classical solution of the problem (3.6). We multiply the PDE of the problem (3.6) by an arbitrary test function $\varphi \in \mathcal{C}_0^1(\mathbb{R} \times [0,\infty))$ and integrate over $\mathbb{R} \times [0,\infty)$. Applying integration by parts, we obtain

$$\begin{aligned} 0 &= \int_{\mathbb{R}} \int_0^\infty (u_t + f(u)_x)\varphi \ \mathrm{d}t\mathrm{d}x \\ &= -\int_{\mathbb{R}} \int_0^\infty (u\varphi_t + f(u)\varphi_x) \ \mathrm{d}t\mathrm{d}x - \int_{\mathbb{R}} u(x,0)\varphi(x,0) \ \mathrm{d}x. \end{aligned}$$

Since φ is compactly supported, other boundary terms disappear. Now we are ready for defining the weak solution.

Definition 6 (Weak solution)**.** *The function $u \in L^1_{loc}(\mathbb{R} \times [0,\infty))$ is called a weak solution of the problem (3.6) if*

$$\int_{\mathbb{R}} \int_0^\infty (u\varphi_t + f(u)\varphi_x) \ \mathrm{d}t\mathrm{d}x = -\int_{\mathbb{R}} u_0(x)\varphi(x,0) \ \mathrm{d}x \tag{3.7}$$

holds $\forall \varphi \in \mathcal{C}_0^1(\mathbb{R} \times [0,\infty))$.

This definition clearly allows discontinuous solutions. It is easy to show that each classical solution is a weak solution. The inverse of this property does not need to be true.

3.1.2 Shock waves and rarefaction waves

Our question is if every kind of discontinuities are allowed. Suppose we have a discontinuity along a curve $s(t)$ in the x-t plane. This curve is called a *shock wave*. At the time t, we take the interval $[x_1,x_2]$ such that $s(t) \in [x_1,x_2]$. In the case of discontinuities, we use the notations $u(s(t)_-,t) = u_l(t)$ and $u(s(t)_+,t) = u_r(t)$. Because problem (3.6) is a conservation law, we know that

$$\frac{\mathrm{d}}{\mathrm{d}t} \int_{x_1}^{x_2} u(x,t) \ \mathrm{d}x = f(u(x_1,t)) - f(u(x_2,t)) \tag{3.8}$$

where the left-hand side is the change of amount of u with respect to time and the right-hand side is difference between inflow and outflow. Now we rewrite the left-hand side of equation (3.8)

$$\begin{aligned} \frac{\mathrm{d}}{\mathrm{d}t} \int_{x_1}^{x_2} u(x,t) \ \mathrm{d}x &= \frac{\mathrm{d}}{\mathrm{d}t} \left(\int_{x_1}^{s(t)} u(x,t) \ \mathrm{d}x + \int_{s(t)}^{x_2} u(x,t) \ \mathrm{d}x \right) \\ &= \int_{x_1}^{s(t)} u_t(x,t) \ \mathrm{d}x + u_l(t)s'(t) + \int_{s(t)}^{x_2} u_t(x,t) \ \mathrm{d}x - u_r(t)s'(t). \end{aligned}$$

On the other side of equation (3.8) we have

$$\begin{aligned} f(u(x_1,t)) - f(u(x_2,t)) &= f(u(x_1,t)) \mp f(u_l(t)) \pm f(u_r(t)) - f(u(x_2,t)) \\ &= -\int_{x_1}^{s(t)} f(u(x,t))_x \ \mathrm{d}x - \int_{s(t)}^{x_2} f(u(x,t))_x \ \mathrm{d}x \\ &\quad + f(u_l(t)) - f(u_r(t)). \end{aligned}$$

According to problem (3.6) and Lemma 1 we obtain

$$\int_{x_1}^{s(t)} u_t(x,t)\ \mathrm{d}x = -\int_{x_1}^{s(t)} f(u(x,t))_x\ \mathrm{d}x$$

and

$$\int_{s(t)}^{x_2} u_t(x,t)\ \mathrm{d}x = -\int_{s(t)}^{x_2} f(u(x,t))_x\ \mathrm{d}x.$$

Finally, we obtain the so called *Rankine-Hugoniot Jump condition*

$$s'(t) = \frac{f(u_l(t)) - f(u_r(t))}{u_l(t) - u_r(t)}.$$

We call $s'(t)$ the *shock speed*.

We can use shock waves for the domains where we have intersection of characteristics. As example we can use Riemann problem from Figure 3.3 (Example 3). If we use the Rankine-Hugoniot Jump condition, we obtain $s'(t) = 0$. Thus $s(t) = 0$ for all $t > 0$. We can see the result in Figure 3.5, where the shock wave is a red line. Now the values $u(x,t)$ are well defined for all $x \in \mathbb{R}$, $t > 0$ by characteristics. Similarly, we can find a well-defined solution for the initial condition from Figure 3.4a (Example 4).

In the case of the Riemann problem from Figure 3.2 (Example 2), we still do not receive unique solution. We can choose the number of jumps. In Figure 3.6, we can see the characteristics. One jump solution has jump from $u_l = 1$ to

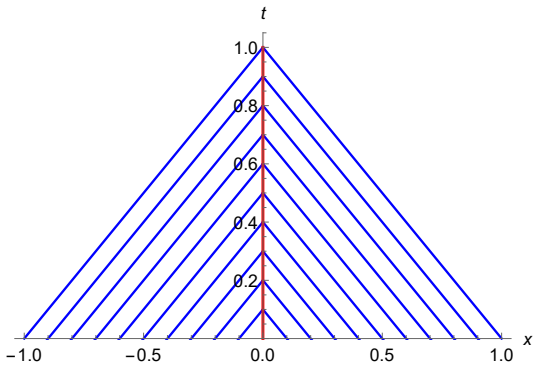

Figure 3.5: Example 3 with the shock wave.

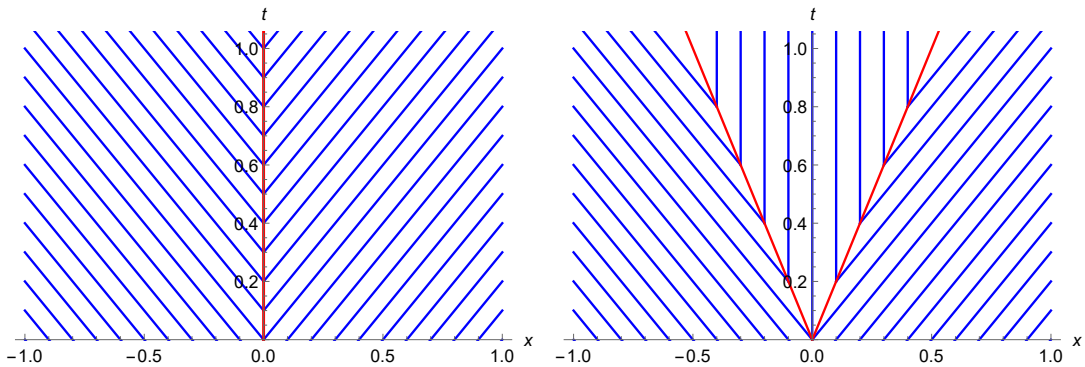

(a) One jump. (b) Two jumps.

Figure 3.6: Example 2 with the shock wave.

$u_r = 0$. The solution with two jumps has first jump from $u_l = 1$ to $u_m = 0.5$ and second jump from $u_m = 0.5$ to $u_r = 0$. Shock waves are red lines in both cases.

In Figure 3.2 (Example 2) we have a domain without characteristics. Thus, at the time t we obtain the interval $(x_1(t),x_2(t))$, where the solution is not defined by characteristics. Assume that the number of jumps tends to $+\infty$. Then we obtain the line, called *rarefaction wave*, which connect the values $u(x_1(t),t)$ and $u(x_2(t),t)$. The solution become continuous, but not differentiable. We can see the result in Figure 3.7. The red lines are the characteristics created by the rarefaction wave.

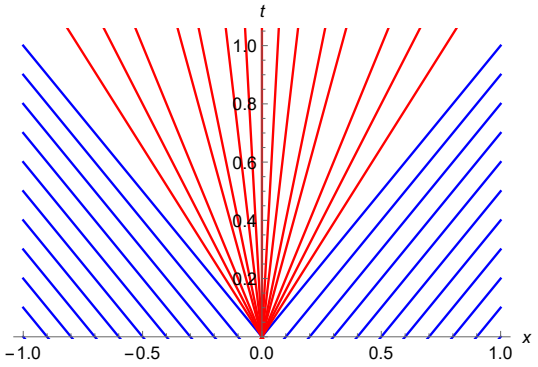

Figure 3.7: Example 2 with the rarefaction wave.

3.1.3 Entropy solution

As we can observe, we do not have the uniqueness of the solution of the problem (3.6). We need other conditions which ensure the uniqueness. The basic condition is called the *limit of small viscosity*. We consider a modified problem

$$\begin{aligned} (u_\epsilon)_t + f\,(u_\epsilon)_x &= \epsilon (u_\epsilon)_{xx}, \qquad x \in \mathbb{R},\, t > 0, \\ u_\epsilon(x,0) &= u_0(x), \qquad x \in \mathbb{R}. \end{aligned} \tag{3.9}$$

This problem has a unique solution u_ϵ for all $\epsilon > 0$. We accept the solution u of the problem (3.6) which can be obtained as a limit of solutions u_ϵ of the problem (3.9) as ϵ tends to 0.

We mention two other entropy conditions. One of them is the *Oleinik entropy condition*

$$\exists c > 0, \forall x \in \mathbb{R}, \forall t \in (0,\infty), \forall z \in [0,\infty) : \; u(x+z,t) - u(x,t) \leq c\left(1 + \frac{1}{t}\right) z, \tag{3.10}$$

which was introduced by Oleinik in [11]. Now we define the *entropy solution*.

Definition 7 (Entropy solution)**.** *Let $f : \mathbb{R} \to \mathbb{R}$ be a concave up function. Then a function $u \in L^1_{loc}(\mathbb{R} \times [0,\infty))$ is called an entropy solution of the problem (3.6) if u is a weak solution, i.e. equation (3.7) holds for all $\varphi \in \mathcal{C}^1_0(\mathbb{R} \times [0,\infty))$, and if the Oleinik entropy condition (3.10) is satisfied almost everywhere in x and t.*

The entropy solution is important for us, because under some assumptions, we can prove the uniqueness of this solution.

Theorem 2 (Uniqueness of the entropy solution)**.** *Let $u_0 \in L^\infty(\mathbb{R})$ and $f \in \mathcal{C}^2$ be uniformly concave up, i.e. there exists $c > 0$ such that $f''(u) \geq c$. Then there exists a unique entropy solution of the problem (3.6).*

Proof. We do not prove this theorem. There are at least three different approaches how to prove it. We can find two of them in the book by Evans [12]. □

The second condition is called the *Lax entropy condition*, which was presented in [13]. This condition says that only those discontinuities where the characteristics go into the shock (like in Figure 3.5) are allowed. Discontinuities where characteristics are generated by the shock (like Figure 3.6) are not allowed. The explanation is that characteristic curves only transport information, which can be destroyed, but they do not create it. The Lax entropy condition can be written mathematically as

$$f'(u_l) > s' > f(u_r),$$

where s' denotes the shock speed.

It can be shown that the limit of small viscosity satisfies the other mentioned entropy conditions.

3.1.4 Traffic context

Now, we would like to apply all the theory above to our traffic problem (3.5). Assume that we have equilibrium quantities satisfying equation (1.3). Then our traffic problem is written as

$$\begin{aligned} \rho_t + Q_e(\rho)_x &= 0, \qquad x \in \mathbb{R},\, t > 0, \\ \rho(x,0) &= \rho_0(x), \qquad x \in \mathbb{R}. \end{aligned} \tag{3.11}$$

As we could notice in Section 1.3, equilibrium traffic flow is typically concave down. Thus, our function "f" is concave down and we cannot use the Oleinik entropy condition (see conditions of Definition 7) and the assumption on f in the uniqueness theorem (Theorem 2) does not hold. That is the reason why we set $u = -\rho$ and define function $F : \mathbb{R} \to \mathbb{R}$, $F(u) := -Q_e(-u) = -Q_e(\rho)$. We multiply traffic problem (3.11) by (-1) and obtain a new problem

$$\begin{aligned} u_t + F(u)_x &= 0, \qquad x \in \mathbb{R},\, t > 0, \\ u(x,0) &= -\rho_0(x), \qquad x \in \mathbb{R}. \end{aligned}$$

Due to $F''(u) = -Q_e''(-u) = -Q_e''(\rho)$, the function F is concave up if Q_e is concave down. Now we can apply the theory above. We have the entropy condition and Definition 7. If Q_e is uniformly concave down, function F is uniformly concave up and we can show the uniqueness of entropy solution u by Theorem 2. Thus, the solution $\rho = -u$ is the unique entropy solution.

There exists a special *traffic entropy condition* presented by Ansorge [14]. This condition says that whenever cars drive into denser traffic then there should be no smoothing (i.e. no rarefaction waves). On the other hand, whenever cars drive into less dense traffic then there should be taken the smoothest solution (i.e. rarefaction waves). Unfortunately, we do not obtain anything new when we compare the traffic entropy condition to the Lax entropy condition.

3.2 Traffic flow models

In this section we introduce macroscopic traffic models. We follow the book by Kachroo and Sastry [10].

We proceed from conservation equation (3.5), where we have unknowns $\rho(x,t)$ and $V(x,t)$. Our aim is to look for the second equation. There is a lot of approaches how to obtain it.

3.2.1 Lighthill-Whitham-Richards model

The Lighthill-Whitham-Richards model (abbreviated LWR) is an approach where we use the equilibrium velocity. Thus, we have only one unknown ρ and we do not need another equation. Our problem is written as

$$\begin{aligned} \rho_t + (\rho V_e(\rho))_x = 0, \qquad & x \in \mathbb{R},\, t > 0, \\ \rho(x,0) = \rho_0(x), \qquad & x \in \mathbb{R}, \end{aligned} \tag{3.12}$$

There are a lot of different proposals for the equilibrium velocity V_e derived from the real traffic data.

Greenshields model This model uses a linear relationship between traffic density and traffic velocity. The equilibrium velocity is given by

$$V_e(\rho) = v_{\max}\left(1 - \frac{\rho}{\rho_{\max}}\right),$$

where $v_{\max}$ is the maximal velocity and $\rho_{\max}$ is the maximal density. We can see the fundamental diagram in Figure 3.8, where $v_{\max} = \rho_{\max} = 1$.

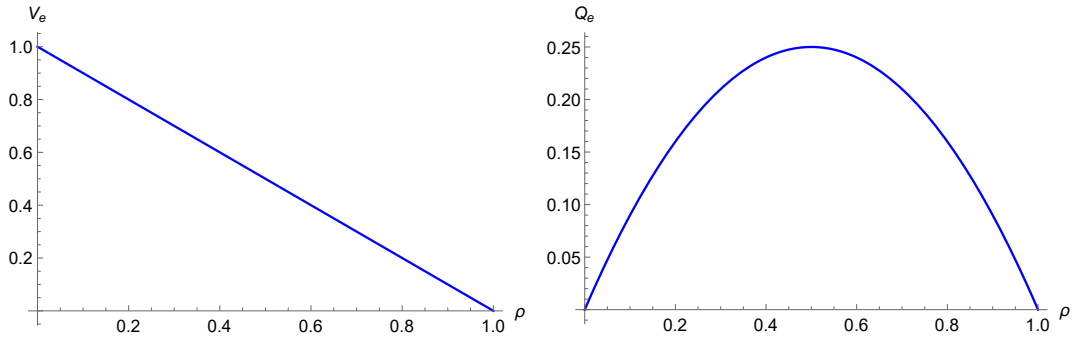

(a) Velocity-density diagram. (b) Flow-density diagram.

Figure 3.8: Fundamental diagrams of the Greenshields model.

Greenberg model This model uses the equilibrium velocity represented by the logarithmic function. Thus, we can overcome the maximal velocity $v_{\max}$. The equilibrium velocity is given by

$$V_e(\rho) = v_{\max} \ln\left(\frac{\rho_{\max}}{\rho}\right),$$

where $v_{\max}$ is the maximal velocity and $\rho_{\max}$ is the maximal density. We can see the fundamental diagram in Figure 3.9, where $v_{\max} = \rho_{\max} = 1$.

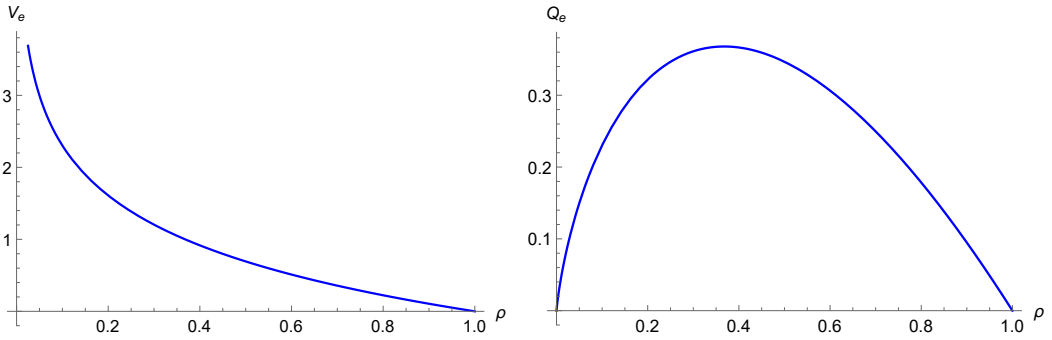

(a) Velocity-density diagram. (b) Flow-density diagram.

Figure 3.9: Fundamental diagrams of the Greenberg model.

Underwood model This model uses the equilibrium velocity represented by the exponential function. Thus, we do not obtain zero velocity at the maximal density $\rho_{\max}$. The equilibrium velocity is given by

$$V_e(\rho) = v_{\max} \exp\left(\frac{-\rho}{\rho_{\max}}\right),$$

where $v_{\max}$ is the maximal velocity and $\rho_{\max}$ is the maximal density. We can see the fundamental diagram in Figure 3.10, where $v_{\max} = \rho_{\max} = 1$. The maximal equilibrium traffic flow Q_e is reached at maximal density $\rho_{\max}$.

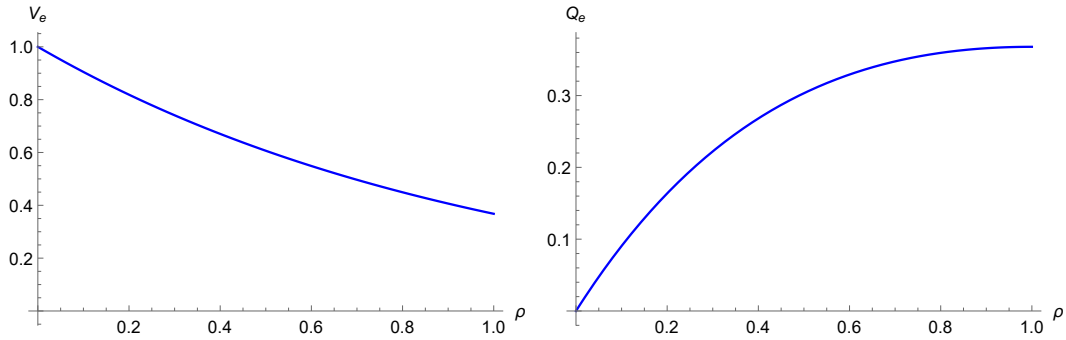

(a) Velocity-density diagram. (b) Flow-density diagram.

Figure 3.10: Fundamental diagrams of the Underwood model.

Diffusion model This model is derived from the Greenshields model. The equilibrium velocity depends not only on the traffic density but also on the derivative of the traffic density. The equilibrium velocity is given by

$$V_e(\rho) = v_{\max}\left(1 - \frac{\rho}{\rho_{\max}}\right) - \frac{D}{\rho}\frac{\partial \rho}{\partial x},$$

where $v_{\max}$ is the maximal velocity, $\rho_{\max}$ is the maximal density and D is a diffusion coefficient. The coefficient is given by $D = \tau v_{\text{rand}}^2$, where τ is a relaxation parameter and v_{rand} is a random velocity.

Other models There exists a lot of different types of models. Most of them are based on real traffic data. We are looking for the approximation of the velocity--density relationships.

3.2.2 Payne-Whitham model

The Payne-Whitham model (abbreviated PW) is an approach where we use two PDEs to represent the traffic dynamics. The second equation is analogous to the fluid momentum equation. We still use the equilibrium velocity. In the most general form, our problem is described by the system

$$\begin{aligned} \rho_t + (\rho V)_x &= 0, \\ V_t + VV_x &= \frac{V_e(\rho) - V}{\tau} - \frac{(A(\rho))_x}{\rho} + \mu \frac{V_{xx}}{\rho}, \end{aligned} \tag{3.13}$$

where $\frac{V_e(\rho)-V}{\tau}$ is a relaxation term, $\frac{(A(\rho))_x}{\rho}$ is an anticipation term and $\mu\frac{V_{xx}}{\rho}$ is a viscosity term. Let us remind that $V_e(\rho)$ is an equilibrium velocity (e.g. from LWR models) and τ is a relaxation time.

The anticipation term is similar to the pressure term in fluids. In some specific models the term is taken as $A(\rho) = c_0^2\rho$ for some constant c_0. If we ignore the viscosity term in the system (3.13), then we obtain the PW model similar to isothermal flow as

$$\begin{aligned} \rho_t + (\rho V)_x &= 0, \\ V_t + VV_x &= \frac{V_e(\rho) - V}{\tau} - \frac{(c_0^2\rho)_x}{\rho}. \end{aligned}$$

Now, our aim is to calculate eigenvalues and eigenvectors of the system (3.13). We need them for studying the characteristics and direction of transport of information. Moreover, we use eigenvalues later in the calculation of numerical flux (Subsection 4.2.2). First, we transform the system (3.13) into the vector form

$$u_t + f(u)_x = S,$$

where

$$u = \begin{bmatrix} \rho \\ \rho V \end{bmatrix}, \qquad f(u) = \begin{bmatrix} \rho V \\ \rho V^2 + c_0^2\rho \end{bmatrix}, \qquad S = \begin{bmatrix} 0 \\ \rho\dfrac{V_e(\rho) - V}{\tau} + \mu V_{xx} \end{bmatrix}.$$

We can write this linear form as

$$u_t + A(u)u_x = S,$$

where

$$A(u) = \frac{\partial f}{\partial u} = \begin{bmatrix} 0 & 1 \\ c_0^2 - V^2 & 2V \end{bmatrix}.$$

The two eigenvalues of the matrix $A(u)$ are $\lambda_1 = V + c_0$ and $\lambda_2 = V - c_0$ and the corresponding eigenvectors are

$$v_1 = \begin{bmatrix} 1 \\ V + c_0 \end{bmatrix} \quad \text{and} \quad v_2 = \begin{bmatrix} 1 \\ V - c_0 \end{bmatrix}.$$

There are a lot of disadvantages to the PW model. One of them is that the PW model imitates the fluid behaviour too closely. Especially the fact that it shows isotropic behaviour, while the traffic behaviour should by anisotropic. Isotropic models exhibit that disturbances can travel in both directions. On the other hand, for vehicular traffic, the driver behaviour should be affected by what happens in front of the car and not in the back.

3.2.3 Aw-Rascle model

The Aw-Rascle model (abbreviated AR) is an approach where we model the anisotropic traffic behaviour. We still use the equilibrium velocity. Our problem is described by the system

$$\rho_t + (\rho V)_x = 0,$$
$$(V + p(\rho))_t + V(V + p(\rho))_x = \frac{V_e(\rho) - V}{\tau}.$$

The pressure term is usually taken as

$$p(\rho) = \rho^\gamma$$

where $\gamma > 0$.

For further analysis, we ignore the relaxation term. We define the new variable $m = \rho(V + p(\rho))$. Then we transform the system into the vector form

$$u_t + f(u)_x = 0,$$

where

$$u = \begin{bmatrix} \rho \\ m \end{bmatrix}, \qquad f(u) = \begin{bmatrix} m - \rho p \\ \dfrac{m^2}{\rho} - mp \end{bmatrix}.$$

We can write this linear form as

$$u_t + A(u)u_x = 0,$$

where

$$A(u) = \frac{\partial f}{\partial u} = \begin{bmatrix} -(\gamma+1)p & 1 \\ -\dfrac{m^2}{\rho^2} - \dfrac{\gamma p m}{\rho} & \dfrac{2m}{\rho} - p \end{bmatrix}.$$

The two eigenvalues of the matrix $A(u)$ are $\lambda_1 = V$ and $\lambda_2 = V - \gamma p$ and the corresponding eigenvectors are

$$v_1 = \begin{bmatrix} 1 \\ V + (\gamma+1)p \end{bmatrix} \quad \text{and} \quad v_2 = \begin{bmatrix} 1 \\ V + p \end{bmatrix}.$$

3.2.4 Zhang model

The Zhang model is an approach where we use an equation derived from a microscopic car following model. This method is called the *micro-macro link* and we present it later in Section 3.3. Our problem is described by the system

$$\rho_t + (\rho V)_x = 0,$$
$$V_t + (V + \rho V_e'(\rho))V_x = \frac{V_e(\rho) - V}{\tau}.$$

For further analysis, we ignore the relaxation term. We define the new variable $m = \rho(V - V_e(\rho))$. Then we transform the system into the vector form

$$u_t + f(u)_x = 0,$$

where

$$u = \begin{bmatrix} \rho \\ m \end{bmatrix}, \qquad f(u) = \begin{bmatrix} m + \rho V_e(\rho) \\ \dfrac{m^2}{\rho} + mV_e(\rho) \end{bmatrix}.$$

We can write this linear form as

$$u_t + A(u)u_x = 0,$$

where

$$A(u) = \frac{\partial f}{\partial u} = \begin{bmatrix} \rho V_e'(\rho) + V_e(\rho) & 1 \\ -\dfrac{m^2}{\rho^2} + mV_e'(\rho) & \dfrac{2m}{\rho} + V_e(\rho) \end{bmatrix}.$$

The two eigenvalues of the matrix $A(u)$ are $\lambda_1 = V$ and $\lambda_2 = V + \rho V_e'(\rho)$ and the corresponding eigenvectors are

$$v_1 = \begin{bmatrix} 1 \\ V - V_e(\rho) - \rho V_e'(\rho) \end{bmatrix} \quad \text{and} \quad v_2 = \begin{bmatrix} 1 \\ V - V_e(\rho) \end{bmatrix}.$$

3.3 Micro-macro link

As we mention above, conservation law gives us one equation (3.5) with two unknowns. So, we need to use a second equation. There are a lot of different options for choosing it. Section 3.2 gives us some examples how to choose it, but these are not all the possibilities. In this section we introduce the method called micro-macro link. This method takes ODEs from the microscopic model and adds it to equation (3.5) in the macroscopic model. The advantage is that we can bring some behaviour of the microscopic models into the macroscopic one. We follow the lecture by Gasser.

We demonstrate the micro-macro link on two microscopic models

a) $v_i(t) = V_{\text{opt}}\left(x_{i+1}(t) - x_i(t)\right)$,

b) $\dfrac{\mathrm{d}v_i}{\mathrm{d}t}(t) = \dfrac{1}{\tau}\left(V_{\text{opt}}\left(x_{i+1}(t) - x_i(t)\right) - v_i(t)\right)$.

The model a) represents the fact that the velocity of car is equal to the optimal velocity. This model is primitive, and we use it to show that we don't need an ODE in this case. Consequently, we do not obtain a second PDE but the definition of function V in equation (3.5). This is similar to LWR models. The model b) is the Bando model (2.1).

3.3.1 Scaling

The choice of a suitable scaling of the quantities is very important. We define reference values

$$v_r = v_{\max}, \qquad t_r = \frac{L}{v_r}, \qquad \rho_r = \frac{1}{l},$$

where $v_{\max}$ is the maximal velocity, L is the length of the road and l is the length of a car. The traffic density is given by

$$\rho\left(\frac{x_{i+1}(t) + x_i(t)}{2}, t\right) = \frac{1}{x_{i+1}(t) - x_i(t)}. \tag{3.14}$$

The connection between an optimal velocity $V_{\text{opt}}(y)$ from the microscopic model and an equilibrium velocity $V_e(\rho)$ from the macroscopic model is given by

$$V_e\left(\rho\left(\frac{x_{i+1}(t) + x_i(t)}{2}, t\right)\right) = V_{\text{opt}}\left(x_{i+1}(t) - x_i(t)\right).$$

Now we are ready to calculate the scaled models a) and b). We use

$$\tilde{t} = \frac{t}{t_r}, \qquad \tilde{\tau} = \frac{\tau}{t_r}, \qquad \epsilon = \tilde{l} = \frac{l}{L},$$

$$\tilde{\rho}\left(\frac{\tilde{x}_{i+1}(\tilde{t}) + \tilde{x}_i(\tilde{t})}{2}, \tilde{t}\right) = \frac{1}{\rho_r}\,\rho\left(\frac{x_{i+1}(t) + x_i(t)}{2}, t\right), \tag{3.15}$$

$$\tilde{x}_i(\tilde{t}) = \frac{1}{L}x_i(\tilde{t}t_r), \qquad \tilde{v}_i(\tilde{t}) = \frac{1}{v_r}v_i(\tilde{t}t_r), \qquad \tilde{V}_e(\tilde{\rho}) = \frac{1}{v_r}V_e(\tilde{\rho}\rho_r)$$

and obtain

a) $\tilde{v}_i(\tilde{t}) = \tilde{V}_e\left(\tilde{\rho}\left(\frac{\tilde{x}_{i+1}(\tilde{t}) + \tilde{x}_i(\tilde{t})}{2}, \tilde{t}\right)\right)$,

b) $\frac{\mathrm{d}\tilde{v}_i}{\mathrm{d}\tilde{t}}(\tilde{t}) = \frac{1}{\tilde{\tau}}\left(\tilde{V}_e\left(\tilde{\rho}\left(\frac{\tilde{x}_{i+1}(\tilde{t}) + \tilde{x}_i(\tilde{t})}{2}, \tilde{t}\right)\right) - \tilde{v}_i(\tilde{t})\right)$.

One can notice that we can use equation (3.14) and apply it to equation (3.15). Then we obtain

$$\begin{aligned}
\tilde{\rho}\left(\frac{\tilde{x}_{i+1}(\tilde{t}) + \tilde{x}_i(\tilde{t})}{2}, \tilde{t}\right) &= \frac{1}{\rho_r}\,\rho\left(\frac{x_{i+1}(t) + x_i(t)}{2}, t\right) \\
&= \frac{1}{\rho_r}\,\frac{1}{x_{i+1}(t) - x_i(t)} \\
&= l\,\frac{1}{L\tilde{x}_{i+1}(\tilde{t}) - L\tilde{x}_i(\tilde{t})} \\
&= \frac{l}{L}\,\frac{1}{\tilde{x}_{i+1}(\tilde{t}) - \tilde{x}_i(\tilde{t})} \\
&= \epsilon\,\frac{1}{\tilde{x}_{i+1}(\tilde{t}) - \tilde{x}_i(\tilde{t})}.
\end{aligned} \tag{3.16}$$

3.3.2 Transformation

Now we have everything prepared for the transformation from a scaled microscopic model to the macroscopic model. For simplicity, we omit tildes in this whole subsection and we use the notation $\rho = \rho(x,t)$, $V = V(x,t)$.

We must introduce new independent variables x and t. We approximate

$$x \approx x_i(t), \qquad V(x,t) \approx v_i(t).$$

According to equation (3.16), we obtain the continued fraction

$$\begin{aligned}
\rho\left(\frac{x_{i+1}(t)+x_i(t)}{2}, t\right) &= \rho\left(x_i(t) + \frac{x_{i+1}(t)-x_i(t)}{2}, t\right) \\
&= \rho\left(x_i(t) + \frac{\epsilon}{2\rho\left(x_i(t)+\frac{\epsilon}{2\rho(\dots)}\right)}, t\right) \\
&\approx \rho\left(x + \frac{\epsilon}{2\rho\left(x+\frac{\epsilon}{2\rho(\dots)}\right)}, t\right). \qquad (3.17)
\end{aligned}$$

We expend continued fraction (3.17) in powers of ϵ and obtain

$$\begin{aligned}
\rho\left(\frac{x_{i+1}(t)+x_i(t)}{2}, t\right) &\approx \rho\left(x + \frac{\epsilon}{2\left(\rho + \frac{\epsilon}{2\rho}\rho_x + \mathcal{O}\left(\epsilon^2\right)\right)}, t\right) \\
&= \rho\left(x + \frac{\epsilon}{2\rho}\left(1 - \frac{\epsilon}{2\rho^2}\rho_x + \mathcal{O}\left(\epsilon^2\right)\right), t\right) \\
&= \rho + \frac{\epsilon}{2\rho}\rho_x - \frac{\epsilon^2}{4\rho^3}\rho_x^2 + \frac{\epsilon^2}{8\rho^2}\rho_{xx} + \mathcal{O}\left(\epsilon^3\right) \\
&= \rho + \frac{\epsilon}{2\rho}\rho_x + \frac{\epsilon^2}{8\rho^2}\left(\rho_{xx} - 2\frac{\rho_x^2}{\rho}\right) + \mathcal{O}\left(\epsilon^3\right). \qquad (3.18)
\end{aligned}$$

Since we have the approximate density (3.18), we can expand the equilibrium velocity in powers of ϵ in the same way and obtain

$$\begin{aligned}
V_e\left(\rho\left(\frac{x_{i+1}(t)+x_i(t)}{2}, t\right)\right) &\approx V_e(\rho) + V_e'(\rho)\left(\frac{\epsilon}{2\rho}\rho_x + \frac{\epsilon^2}{8\rho^2}\left(\rho_{xx} - 2\frac{\rho_x^2}{\rho}\right)\right) \\
&\quad + V_e''(\rho)\frac{\epsilon^2\rho_x^2}{8\rho^2} + \mathcal{O}\left(\epsilon^3\right) \\
&= V_e(\rho) + \epsilon V_e'(\rho)\frac{\rho_x}{2\rho} + \frac{\epsilon^2}{8\rho^2}\left(V_e'(\rho)\left(\rho_{xx} - 2\frac{\rho_x^2}{\rho}\right)\right. \\
&\quad \left. + V_e''(\rho)\rho_x^2\right) + \mathcal{O}\left(\epsilon^3\right) \\
&= V_e(\rho) + \frac{\epsilon}{2\rho}V_e(\rho)_x + \frac{\epsilon^2}{8\rho^2}\left(V_e(\rho)_{xx} - 2V_e(\rho)_x\frac{\rho_x}{\rho}\right) \\
&\quad + \mathcal{O}\left(\epsilon^3\right).
\end{aligned}$$

Finally, we must approximate the left-hand side of the Bando model. We can develop velocity in power of Δt and obtain

$$\begin{aligned}\frac{\mathrm{d}v_i}{\mathrm{d}t}(t) &= \lim_{\Delta t\to 0}\frac{v_i(t+\Delta t)-v_i(t)}{\Delta t}\\ &\approx \lim_{\Delta t\to 0}\frac{V(x+V\Delta t,t+\Delta t)-V}{\Delta t}\\ &= \lim_{\Delta t\to 0}\frac{V+V_xV\Delta t+V_t\Delta t+\mathcal{O}\left((\Delta t)^2\right)-V}{\Delta t}\\ &= V_t+VV_x.\end{aligned}$$

Using these calculations, we can approximate scaled microscopic models a) and b) and get the missing equation in macroscopic model. From the microscopic model a) we obtain the scalar second order equation

$$\rho_t+\left(\rho V_e(\rho)\right)_x=-\frac{\epsilon}{2}V_e(\rho)_{xx}+\mathcal{O}\left(\epsilon^2\right).$$

From the Bando model b) we obtain the first order systems of balance equations

$$\begin{aligned}\rho_t+\left(\rho V\right)_x&=0\\ V_t+VV_x&=\frac{1}{\tau}\left(V_e(\rho)-V+\frac{\epsilon}{2\rho}V_e(\rho)_x\right)+\mathcal{O}\left(\epsilon^2\right).\end{aligned}$$

We use approximation up to first order in powers of ϵ. On a short road, i.e. when ϵ is large, we must use higher order and we obtain more complicated equations.

3.4 Junctions

This section follows the book by Garavello and Piccoli [15]. We study a complex network represented by a directed graph. The graph is a finite collection of directed edges, connected together at some vertices. Each vertex has a finite set of incoming edges and outgoing edges. First, we define the *network*.

Definition 8 (Network)**.** *We define a network as a couple $(\mathcal{I},\mathcal{J})$, where $\mathcal{I}=\{I_n\}_{n=1}^N$ is a finite set of edges and $\mathcal{J}=\{J_m\}_{m=1}^M$ is a finite set of vertices. Each edge I_n is an interval $[a_i,b_i]\subseteq[-\infty,\infty]$, $i=1,\dots,N$. Each vertex J_m is a union of two non-empty subsets $Inc(J_m)$ and $Out(J_m)$ of $\{1,\dots,N\}$. We assume the following:*

(i) $\forall J_i,J_j\in\mathcal{J},\ i\neq j:(Inc(J_i)\cap Inc(J_j)=\emptyset)\wedge(Out(J_i)\cap Out(J_j)=\emptyset)$.

(ii) If $i\notin\cup_{J\in\mathcal{J}}Inc(J)$, $i\in\{1,\dots,N\}$, then $b_i=\infty$ and if $i\notin\cup_{J\in\mathcal{J}}Out(J)$, $i\in\{1,\dots,N\}$, then $a_i=-\infty$. Moreover, $\forall i\in\{1,\dots,N\}:(i\in\cup_{J\in\mathcal{J}}Inc(J))\vee(i\in\cup_{J\in\mathcal{J}}Out(J))$.

The two conditions define the network as a graph. Condition (i) implies that each edge can be incoming for at most one vertex and outgoing for at most vertex. Condition (ii) implies that some edges may extend to infinity but are connected to at least one vertex. We can see an example in Figure 3.11.

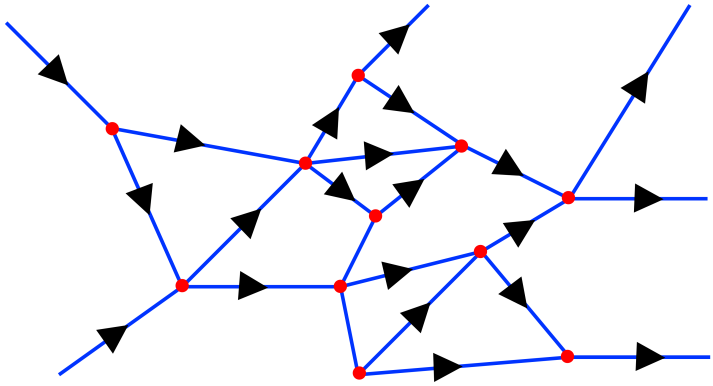

Figure 3.11: Example of a network.

If we want to find a solution on a network, we need to solve the same problem on each edge and at each vertex. Because it is enough to extend the problem from one vertex and its incoming and outgoing edges to all vertices and all edges, we will study our problem only at one vertex and on its incoming and outgoing edges.

3.4.1 Riemann solver

In this subsection, we assume that the traffic on edge number $i \in \{1,\dots,N\}$ is represented by the hyperbolic system

$$\begin{aligned} (u_i)_t + f_i\,(u_i)_x = 0, \qquad & x \in \mathbb{R},\ t > 0, \\ u_i(x,0) = u_{i,0}(x), \qquad & x \in \mathbb{R}, \end{aligned} \tag{3.19}$$

where $f_i : \mathbb{R}^p \to \mathbb{R}^p$. Now we fix $(\mathcal{I},\mathcal{J})$ and a vertex $J \in \mathcal{J}$ and assume that $\mathrm{Inc}(J) = \{1,\dots,n\}$ and $\mathrm{Out}(J) = \{n+1,\dots,n+m\}$. We would like to define and solve the *Riemann problems* at vertices.

Definition 9 (Riemann problem at a vertex)**.** *The problem (3.19) with initial data which are constant on each edge is called a Riemann problem.*

Now we define a *Riemann solver*.

Definition 10 (Riemann solver for a vertex)**.** *We define a Riemann solver for the vertex J as a function*

$$RS : (\mathbb{R}^p)^{n+m} \to (\mathbb{R}^p)^{n+m}$$

that associates to every Riemann datum $u_0 = (u_{1,0},\dots,u_{n+m,0})^T$ at J a vector $\widehat{u} = (\widehat{u}_1,\dots,\widehat{u}_{n+m})^T$ such that the following holds:

(i) On each edge I_i, $i = 1,\dots,n+m$, the solution is given by the solution to the initial-boundary value problem with initial data $u_{i,0}$ and boundary data $\widehat{u}_i$.

(ii) $RS(RS(u_0)) = RS(u_0)$. This equation is called the consistency condition.

We can say that Riemann solver is a map assigning a solution to each Riemann initial datum.

Since a Riemann solver is defined, we can define admissible solution at J.

Definition 11 (Admissible solution at a vertex)**.** *Assume a Riemann Solver RS is given at junction J. Let* $u = (u_1, \dots, u_{n+m})^T$, $u_i : [a_i, b_i] \times [0, \infty) \to \mathbb{R}^p$ *be such that* $u_i(\cdot, t)$ *is of bounded variation* $\forall t \geq 0$. *Then u is called an admissible weak solution to (3.19) related to RS at the vertex J if the following holds:*

(i) u_i *is a weak solution to (3.19) on the edge.*

(ii) Setting

$$u_J(t) = (u_1(b_{1,-}, t), \dots, u_n(b_{n,-}, t), u_{n+1}(a_{n+1,+}, t), \dots, u_{n+m}(a_{n+m,+}, t))^T,$$

we have $RS(u_J(t)) = u_J(t)$ *for almost every t.*

Unfortunately, this general definition does not give us unique solutions. Moreover, it includes "non-physical" cases. For example, the quantity u, or some components of u, must be conserved also at vertex J. In our traffic case, our u is traffic density. Now, it is possible to create or lose some density in a junction. One necessary condition is to hold equality of incoming and outgoing fluxes for the obtained solution $\widehat{u}$. However, that is still not enough. The initial-boundary value problem on each edge can produce a solution which does not reach the boundary value pointwise. So, the solution to the initial-boundary value problems needs to have negative characteristic velocities on incoming edges and positive characteristic velocities on outgoing edges. In summary, we must satisfy these two conditions

(Condition 1) If $\widehat{u} = RS(u_0)$, then for incoming edges, i.e. $i = 1, \dots, n$, the solution to the Riemann problem $(\widehat{u}_i, u_{i,0},)$ has all waves with strictly negative velocity. On the other hand, for outgoing edges, i.e. $j = n+1, \dots, n+m$, the solution to the Riemann problem $(\widehat{u}_j, u_{j,0})$ has all waves with strictly positive velocity.

(Condition 2) If $\widehat{u} = RS(u_0)$, then the incoming flux is equal to the outgoing one, i.e.

$$\sum_{i=1}^{n} f_i(\widehat{u}_i) = \sum_{j=n+1}^{n+m} f_j(\widehat{u}_j).$$

We can reformulate the second condition to traffic situation as follows: the number of cars which enter the junction is equal to the number of cars which leave the junction.

3.4.2 LWR model on junctions

On each road (edge) we consider the LWR model (mentioned above in Subsection 3.2.1), while at the junctions (vertices) we consider the Riemann solver satisfying the two conditions above and the following rules:

a) There are some prescribed preferences of drivers how the traffic from incoming roads is distributed to outgoing roads according to fixed coefficients.

b) Respecting a), drivers choose so as to maximize fluxes through each junction.

Recall that LWR models solve the problem (3.12) and $Q_e(\rho) = \rho V_e(\rho)$. Assume that $\rho_{\max} = 1$, $Q_e(\rho) \in \mathcal{C}^2$ is a strictly concave down function and $Q_e(0) = Q_e(1) = 0$. At each junction J, there is a matrix describing the distribution of the traffic among outgoing roads.

Definition 12 (Traffic-distribution matrix)**.** *Let J be a fixed vertex with n incoming edges and m outgoing edges. Then we define a traffic-distribution matrix A as*

$$A = \begin{bmatrix} \alpha_{n+1,1} & \cdots & \alpha_{n+1,n} \\ \vdots & \vdots & \vdots \\ \alpha_{n+m,1} & \cdots & \alpha_{n+m,n} \end{bmatrix},$$

where $\forall i \in \{1,\dots,n\}, j \in \{n+1,\dots,n+m\} : \ 0 \le \alpha_{j,i} \le 1$ and $\forall i \in \{1,\dots,n\}$:

$$\sum_{j=n+1}^{n+m} \alpha_{j,i} = 1.$$

The i^{th} column of A describes how the traffic from the incoming road I_i distributes in percentages to the outgoing roads at the junction J. In other words, if X is the quantity of traffic coming from road I_i then $\alpha_{j,i}X$ is the quantity of traffic moving towards road I_j.

We add a third rule to the rules a) and b) from the beginning of this section. This added rule is a technical condition on matrix A.

c) Let $\{e_1,\dots,e_n\}$ be the canonical basis of $\mathbb{R}^n$ and let $\alpha_j = (\alpha_{j,1},\dots,\alpha_{j,n})^T \in \mathbb{R}^n$ for every $j = n+1,\dots,n+m$. Define $H_i = \{e_i\}^\perp$ for every $i = 1,\dots,n$ and define $H_j = \{\alpha_j\}^\perp$ for every $j = n+1,\dots,n+m$. Let $\mathcal{K}$ be a set of indices $k = (k_1,\dots,k_l)$, $1 \le l \le n-1$, such that $0 \le k_1 < k_2 < \dots < k_l \le n+m$ and for every $k \in \mathcal{K}$ set $H_k = \cap_{h=1}^{l} H_{k_h}$. Let $\mathbf{1} = (1,\dots,1)^T$. Then for every $k \in \mathcal{K} : \mathbf{1} \notin H_k^\perp$.

The condition c) is important to isolate a unique solution to Riemann problems at junctions. From c) we immediately derive $m \ge n$. Otherwise, we take $k = \{n+1,\dots,n+m\}$ and obtain $\mathbf{1} = \sum_{j=n+1}^{n+m} \alpha_j$ from Definition 12. Thus, we get $\mathbf{1} \in H_k^\perp$, where

$$H_k = \cap_{j=n+1}^{n+m} H_j = \cap_{j=n+1}^{n+m} \{\alpha_j\}^\perp.$$

If the condition c) does not hold, we introduce further parameters. The case of $n \ge 2$ incoming roads and $m = 1$ outgoing road is described in [15, Subsection 5.2.2, page 103].

Now we are ready to present the definitions of solution at junctions.

Definition 13 (Traffic solution at a junction)**.** *Let J be a junction with incoming roads $I_1,\dots,I_n$ and outgoing road $I_{n+1},\dots,I_{n+m}$. Then we define a weak solution at J as a collection of functions $\rho_l : I_l \times [0,\infty) \to \mathbb{R}$, $l = 1,\dots,n+m$ such that*

$$\sum_{l=1}^{n+m} \left(\int_{a_l}^{b_l} \int_0^\infty \left(\rho_l \frac{\partial \varphi_l}{\partial t} + Q_e(\rho_l) \frac{\partial \varphi_l}{\partial x} \right) \mathrm{d}t\mathrm{d}x \right) = 0$$

holds for every $\varphi_l \in \mathcal{C}_0^1([a_l,b_l] \times [0,\infty))$, $l = 1,\dots,n+m$, that are also smooth across the junction, i.e.

$$\varphi_i(b_{i-},\cdot) = \varphi_j(a_{j+},\cdot), \qquad \frac{\partial \varphi_i}{\partial x}(b_{i-},\cdot) = \frac{\partial \varphi_j}{\partial x}(a_{j+},\cdot),$$

where $i \in \{1,\dots,n\}$ and $j \in \{n+1,\dots,n+m\}$.

Lemma 3. *Let $\rho = (\rho_1, \ldots, \rho_{n+m})^T$ be a weak solution at the junction J such that each $x \to \rho_i(x,t)$ has bounded variation. Then ρ satisfies*

$$\sum_{i=1}^{n} Q_e(\rho_i(b_{i-},t)) = \sum_{j=n+1}^{n+m} Q_e(\rho_j(a_{j+},t)) \tag{3.20}$$

for almost every $t > 0$ at the junction J.

Proof. We do not prove this lemma. We can find the proof in the book [15, Lemma 5.1.9, page 98]. □

The equation (3.20) is called the Rankine-Hugoniot condition. Finally, we formulate the definition of an admissible weak solution.

Definition 14 (Admissible traffic solution at a junction)**.** *Let $\rho = (\rho_1, \ldots, \rho_{n+m})^T$ be such that $\rho_i(\cdot,t)$ is of bounded variation for every $t \geq 0$. Then ρ is called an admissible weak solution of (3.12) related to the matrix A at the junction J if the following properties hold:*

(i) *ρ is a weak solution at the junction J.*

(ii) *$Q_e(\rho_j(a_{j+},\cdot)) = \sum_{i=1}^{n} \alpha_{j,i} Q_e(\rho_i(b_{i-},\cdot))$, $\forall j = n+1, \ldots, n+m$.*

(iii) *$\sum_{i=1}^{n} Q_e(\rho_i(b_{i-},\cdot))$ is a maximum subject to (i) and (ii).*

Due to Lemma 3, the assumption (i) of the previous definition is the conservation of car at junctions. The assumption (ii) describe the condition a) and the assumption (iii) describe the condition b) from the beginning of this subsection.

4. Discontinuous Galerkin method

In this chapter we follow the book by Dolejší, Knobloch, Kučera and Vlasák [16]. Our aim is to study a method which fits perfectly into our traffic problem. Our method must be able to approximate discontinuous solutions of the systems of PDEs. This method should be fast and robust. This is the reason why we choose the *discontinuous Galerkin method*.

4.1 Introduction

The "standard" conforming finite element method (abbreviated FEM) has many advantages and this method is well known and studied. Unfortunately, FEM has the problem called *Gibbs phenomenon*. This phenomenon is manifested by spurious oscillations that are caused by steep gradients and discontinuities in the exact solution.

In 1973, Reed and Hill [17] invented a new numerical scheme called the discontinuous Galerkin finite element method (abbreviated DG) which avoids the Gibbs phenomenon. The method is similar to conforming FEM. We use piecewise polynomial functions, but there are no continuity assumptions between neighbouring elements. Thus, we approximate by piecewise smooth, but globally discontinuous functions. As we will see later in Subsection 4.2.2, we must calculate a *numerical flux*. This is similar to the finite volume method (abbreviated FVM). Hence, DG is a combination of FEM and FVM and it combines their advantages.

Originally, the DG method is described on a polygonal (polyhedral) domain $\Omega \subset \mathbb{R}^d$, $d \in \mathbb{N}$. Since the traffic model is defined on a line, we consider $\Omega \subset \mathbb{R}$, $\Omega = (a,b)$. Let $\mathcal{T}_h$ be a partition of $\overline{\Omega}$ into a finite number of closed elements K with mutually disjoint interiors, such that

$$\overline{\Omega} = \bigcup_{K \in \mathcal{T}_h} K.$$

In the 1D case, an element K is an interval $[a_K, b_K]$, where a_K and b_K are boundary points of K. We set $h_K = |b_K - a_K|$, $h = \max_{K \in \mathcal{T}} h_K$. We denote the set of all boundary points of all elements by $\mathcal{F}_h$. Further, we define the set of all inner points by

$$\mathcal{F}_h^I = \{x \in \mathcal{F}_h;\ x \in \Omega\}$$

and the set of all boundary points by

$$\mathcal{F}_h^B = \{a, b\}.$$

Obviously $\mathcal{F}_h = \mathcal{F}_h^I \cup \mathcal{F}_h^B$.

In the continuous case, we use standard *Sobolev spaces*. Now, we need the space of discontinuous functions. So, we define *broken Sobolev spaces*.

Definition 15 (Broken Sobolev space)**.** *Let $H^k(I)$, $k \in \mathbb{N}$ be the Sobolev space over an interval I and let $\mathcal{T}_h$ be a partition of open interval Ω. Then we define*

the broken Sobolev space over $\mathcal{T}_h$ *as*

$$H^k(\Omega, \mathcal{T}_h) = \{v;\ v|_K \in H^k(K),\ \forall K \in \mathcal{T}_h\}$$

equipped with the seminorm

$$|v|_{H^k(\Omega,\mathcal{T}_h)} = \left(\sum_{K\in\mathcal{T}_h} |v|^2_{H^k(K)} \right)^{\frac{1}{2}}.$$

This space consists of functions which are piecewise Sobolev, i.e. weakly differentiable on separate elements, but which are in general globally discontinuous.

Instead of the broken Sobolev space $H^k(\Omega, \mathcal{T}_h)$, we use approximation of that space. Let $p \geq 0$ be an integer. Then we define the space of discontinuous piecewise polynomial functions as

$$S_h = \{v;\ v|_K \in P^p(K),\ \forall K \in \mathcal{T}_h\},$$

where $P^p(K)$ denotes the space of all polynomials on K of degree at most p.

For each point $x \in \mathcal{F}_h^I$ there exist two neighbours $K_x^{(L)}$, $K_x^{(R)} \in \mathcal{T}_h$ such that $x = K_x^{(L)} \cap K_x^{(R)}$. Every function $v \in H^k$ is generally discontinuous at $x \in \mathcal{F}_h^I$. Thus, we introduce the following notation:

$$v^{(L)}(x) = \lim_{y\to x_-} v(y), \qquad v^{(R)}(x) = \lim_{y\to x_+} v(y),$$
$$\langle v\rangle_x = \frac{1}{2}(v^{(L)}(x) + v^{(R)}(x)), \qquad [v]_x = v^{(L)}(x) - v^{(R)}(x).$$

In the point $x \in \mathcal{F}_h^B$ there are not two neighbours. In order to have consistent notation, we define

$$v^{(R)}(a) = \lim_{y\to a_+} v(y), \qquad v(a) = \langle v\rangle_a = -[v]_a = v^{(L)}(a) := v^{(R)}(a),$$
$$v^{(L)}(b) = \lim_{y\to b_-} v(y), \qquad v(b) = \langle v\rangle_b = [v]_b = v^{(R)}(b) := v^{(L)}(b).$$

The definition of jump $[v]_a := -v^{(R)}(a)$ or $[v]_b := v^{(L)}(b)$ may seem inconsistent with the definition on interior points. This notation is used due to the integration by parts in following sections. Our notation allows us to simplify those terms.

For simplicity, if $\langle\cdot\rangle_x$, $[\cdot]_x$ appear in a sum of the form $\sum_{x\in\mathcal{F}_h} \ldots$, we omit the index x and write $\langle\cdot\rangle$, $[\cdot]$.

4.2 First order hyperbolic problems

We begin with formulating the DG method for first order hyperbolic problems

$$u_t + f(u)_x = g, \qquad x \in \Omega,\ t \in (0,T), \tag{4.1}$$
$$u = u_D, \qquad x \in \mathcal{F}_h^D\ t \in (0,T), \tag{4.2}$$
$$u(x,0) = u_0(x), \qquad x \in \Omega, \tag{4.3}$$

where the right-hand side $g : \Omega \times (0,T) \to \mathbb{R}$, the Dirichlet boundary condition $u_D : \mathcal{F}_h^D \times (0,T) \to \mathbb{R}$ and the initial condition $u_0 : \Omega \to \mathbb{R}$ are given functions. The Dirichlet boundary condition is prescribed only on the inlet $\mathcal{F}_h^D \subseteq \mathcal{F}_h^B$, respecting the direction of information propagation, cf. also Subsection 4.2.2. The function $f \in \mathcal{C}^1(\mathbb{R})$ is called the *convective flux*. Our aim is to seek a function $u : \Omega \times (0,T) \to \mathbb{R}$ such that (4.1)-(4.3) is satisfied. As we have seen, problem (4.1) is the main part of macroscopic equations for traffic.

4.2.1 Formulation

We would like to derive a weak form of equation (4.1). We multiply (4.1) by a test function $\varphi \in H^1(\Omega,\mathcal{T}_h)$ and integrate over arbitrary element $K \in \mathcal{T}_h$. Then we apply integration by parts and obtain

$$\int_K u_t\varphi \,\mathrm{d}x - \int_K f(u)\varphi' \,\mathrm{d}x + f(u(b_K,t))\varphi^{(L)}(b_K) - f(u(a_K,t))\varphi^{(R)}(a_K) = \int_K g\varphi \,\mathrm{d}x. \tag{4.4}$$

Finally, we sum equation (4.4) over all $K \in \mathcal{T}_h$ and obtain

$$\int_\Omega u_t\varphi \,\mathrm{d}x - \sum_{K\in\mathcal{T}_h} \int_K f(u)\varphi' \,\mathrm{d}x + \sum_{x\in\mathcal{F}_h} f(u)\,[\varphi] = \int_\Omega g\varphi \,\mathrm{d}x.$$

Up until now, the function $u : \Omega \times (0,T) \to \mathbb{R}$ was a continuous function. Let us take $u_h \in H^1(\Omega,\mathcal{T}_h)$ which is in general discontinuous in $\mathcal{F}_h$. Thus, we have a problem with function $f(u_h)$ in the point $x \in \mathcal{F}_h$, because u_h does not have a uniquely defined value on $\mathcal{F}_h$. We proceed similarly as in the finite volume method and use the approximation

$$f(u_h) \approx H(u^{(L)},u^{(R)}), \tag{4.5}$$

where $H(u^{(L)},u^{(R)})$ is a numerical flux. We derive the numerical flux later in Subsection 4.2.2. So, a weak form of equation (4.1) on $H^1(\Omega,\mathcal{T}_h)$ is

$$\int_\Omega (u_h)_t\varphi \,\mathrm{d}x - \sum_{K\in\mathcal{T}_h} \int_K f(u_h)\varphi' \,\mathrm{d}x + \sum_{x\in\mathcal{F}_h} H(u^{(L)},u^{(R)})\,[\varphi] = \int_\Omega g\varphi \,\mathrm{d}x. \tag{4.6}$$

Now we can define a *DG finite element solution.*

Definition 16 (DG finite element solution of hyperbolic problem)**.** *The function $u_h : \Omega \times (0,T) \to \mathbb{R}$ is called a DG finite element solution of hyperbolic problem (4.1)-(4.3) if the following properties hold:*

(i) $u_h \in \mathcal{C}^1([0,T]; S_h)$.

(ii) $u_h(0) = u_{h0}$, *where* u_{h0} *denotes an* S_h *approximation of the initial condition* u_0.

(iii) $u_h = u_D$ *for all* $x \in \mathcal{F}_h^D$, $t \in (0,T)$.

(iv) The equation (4.6) holds for all $\varphi \in S_h$ *and for all* $t \in (0,T)$.

4.2.2 Numerical flux

To calculate the left-hand side in equation (4.6), we need use the numerical flux $H(u^{(L)},u^{(R)})$. From (4.5), we know that the numerical flux approximates the convective flux in points $x \in \mathcal{F}_h$. We use upwinding and some of the conservative schemes from the paper by Shu [18] and the lecture notes by Sonnendrücker [19].

The numerical fluxes are thoroughly studied and well understood from the finite volume method. We assume that numerical flux H has the following properties:

a) $H(u,v)$ is consistent:

$$H(u,u) = f(u), \qquad \forall u \in \mathbb{R}.$$

b) $H(u,v)$ is monotone: $H(u,v)$ is a non-decreasing function of its first argument u and a non-increasing function of its second argument v.

c) Whenever f is Lipschitz continuous, $H(u,v)$ is Lipschitz continuous: there exists constant $L > 0$ such that

$$|H(u_1,v_1) - H(u_2,v_2)| \leq L\left(|u_1 - u_2| + |v_1 - v_2|\right), \qquad \forall u_1,u_2,v_1,v_2 \in \mathbb{R}.$$

The obvious choices of numerical flux are

$$H(u^{(L)},u^{(R)}) = \langle f(u_h)\rangle = \frac{f\left(u^{(L)}\right) + f\left(u^{(R)}\right)}{2}$$

or

$$H(u^{(L)},u^{(R)}) = f\left(\langle u_h\rangle\right) = f\left(\frac{u^{(L)} + u^{(R)}}{2}\right).$$

However, it can be shown that these choices lead to unstable schemes. This is caused by the fact that the averaging is natural for diffusive problems, not for convective problems. Thus, we must introduce other schemes which transport the information in the same way as convective terms.

We use the *upwind flux* as the basic numerical flux. We define

$$\alpha = f'\left(\langle u_h\rangle\right) = f'\left(\frac{u^{(R)} + u^{(L)}}{2}\right)$$

Then we calculate the numerical flux as

$$H\left(u^{(L)},u^{(R)}\right) = \begin{cases} f\left(u^{(L)}\right), & \alpha \geq 0, \\ f\left(u^{(R)}\right), & \alpha < 0. \end{cases}$$

This scheme was inspired by the method of characteristics. The slope of the characteristics depends on the derivative of f. Since the positive derivative transports the information to the right, we take the left point $u^{(L)}$ to evaluate f and vice versa.

The second example is the *Lax-Friedrichs flux*. We define

$$\alpha = \max_{u \in \left(u^{(L)},u^{(R)}\right)} |f'(u)|.$$

We assume that interval $\left(u^{(L)},u^{(R)}\right)$ is non-empty, i.e. we take interval $\left(u^{(R)},u^{(L)}\right)$ in the case of $u^{(R)} < u^{(L)}$. In practice, we do not solve the maximization problem. We approximate by calculating $|f'(u)|$ in the points $u^{(L)}$, $u^{(R)}$ and $\frac{u^{(L)}+u^{(R)}}{2}$ and we take the maximal value. Then we calculate the numerical flux as

$$H\left(u^{(L)},u^{(R)}\right) = \frac{1}{2}\left(f\left(u^{(L)}\right) + f\left(u^{(R)}\right) - \alpha\left(u^{(R)} - u^{(L)}\right)\right). \tag{4.7}$$

The last flux is for systems of PDEs. We call it the generalised Lax-Friedrichs flux or the *Rusanov flux*. We must calculate $f'(u)$, which for systems represents the *Jacobi matrix*. We find its eigenvalues $\{\lambda_1(u),\ldots,\lambda_p(u)\}$ and define

$$\alpha = \max_{u\in\left(u^{(L)},u^{(R)}\right)} \max_{k=1,\ldots,p} \left|\lambda_k\left(u\right)\right|,$$

where $\left(u^{(L)},u^{(R)}\right)$ denotes a box $\left(u_1^{(L)},u_1^{(R)}\right)\times\ldots\times\left(u_p^{(L)},u_p^{(R)}\right)$. Again, we assume that intervals $\left(u_i^{(L)},u_i^{(R)}\right)$ are non-empty for all $i=1,\ldots,p$. We do not solve the maximization problem. Again, we approximate by taking $|\lambda_k(u)|$ in the points $u^{(L)}$, $u^{(R)}$ and $\frac{u^{(L)}+u^{(R)}}{2}$ for all $k=1,\ldots,p$ and we take the maximal value. Then we calculate the numerical flux same as the Lax-Friedrichs flux (4.7).

4.3 Second order elliptic problems

The second case is the DG method for second order elliptic problems

$$-u'' = g, \qquad x\in\Omega, \tag{4.8}$$

$$u = u_D, \qquad x\in\mathcal{F}_h^D, \tag{4.9}$$

$$\frac{\partial u}{\partial \mathbf{n}} = g_N, \qquad x\in\mathcal{F}_h^N, \tag{4.10}$$

where the right-hand side $g:\Omega\to\mathbb{R}$ is a given function and the Dirichlet boundary condition $u_D:\mathcal{F}_h^D\to\mathbb{R}$ and the Neumann boundary condition $g_N:\mathcal{F}_h^N\to\mathbb{R}$ are given constants. Sets $\mathcal{F}_h^D\subseteq\mathcal{F}_h^B$ and $\mathcal{F}_h^N\subseteq\mathcal{F}_h^B$ are disjoint and satisfy $\mathcal{F}_h^D\cup\mathcal{F}_h^N=\mathcal{F}_h^B$. Our aim is to seek a function $u:\Omega\to\mathbb{R}$ such that (4.8)-(4.10) is satisfied. We need to solve problem (4.8) in the PW model.

4.3.1 Formulation

We would like to derive a weak form of equation (4.8). Assume that $u\in\mathcal{C}^2(\Omega)$. We multiply (4.8) by a test function $\varphi\in H^2(\Omega,\mathcal{T}_h)$ and integrate over arbitrary element $K\in\mathcal{T}_h$. Then we apply integration by parts and obtain

$$\int_K u'\varphi'\,\mathrm{d}x - u'(b_K,t)\varphi^{(L)}(b_K) + u'(a_K,t)\varphi^{(R)}(a_K) = \int_K g\varphi\,\mathrm{d}x. \tag{4.11}$$

Since u' is continuous, then $u'=\langle u'\rangle$ on $\mathcal{F}_h^I$. Finally, we sum equation (4.11) over all $K\in\mathcal{T}_h$ and obtain

$$\sum_{K\in\mathcal{T}_h}\int_K u'\varphi'\,\mathrm{d}x - \sum_{x\in\mathcal{F}_h^I}\langle u'\rangle\left[\varphi\right] - \sum_{x\in\mathcal{F}_h^D} u'\left[\varphi\right] = \int_\Omega g\varphi\,\mathrm{d}x + \sum_{x\in\mathcal{F}_h^N} g_N\varphi. \tag{4.12}$$

This equation represents a weak formulation of problem (4.8). Unfortunately, the left-hand side of equation (4.12) has several disadvantages:

a) The left-hand side is not symmetric with respect to u and φ.

b) The left-hand side is not elliptic with respect to some suitable energy norm.

c) Equation (4.12) does not include the Dirichlet boundary condition (4.9).

4.3.2 Penalty terms

In order to manage the problem a), we add the term

$$-\Theta \sum_{x\in\mathcal{F}_h^I} \langle\varphi'\rangle\,[u]\,,$$

where Θ is a constant, to the left-hand side. Since the classical solution u satisfies $[u]=0$ on interior points, the new term is identically zero. Thus, we do not affect the consistency with the problem (4.8).

In order to manage the problem c), we add the terms

$$-\Theta \sum_{x\in\mathcal{F}_h^D} \varphi'\,[u] = -\Theta \sum_{x\in\mathcal{F}_h^D} \varphi'\,[u_D]\,,$$

where Θ is a same constant as in the first term. There are three options how to choose Θ.

Remark. Usually, we choose $\Theta = -1,\ 0,\ 1$. $\Theta = 1$ leads to the *symmetric* (abbreviated SIPG), $\Theta = 0$ to *incomplete* (abbreviated IIPG) and $\Theta = -1$ to *nonsymmetric interior penalty Galerkin method* (abbreviated NIPG).

In order to manage the problem b) and c), we add the so-called *interior and boundary penalty terms*

$$C_W \sum_{x\in\mathcal{F}_h^I} [u]\,[\varphi] + C_W \sum_{x\in\mathcal{F}_h^D} u\varphi = C_W \sum_{x\in\mathcal{F}_h^D} u_D\varphi,$$

where $C_W > 0$ is a constant, which provides ellipticity of the resulting form.

Up until now, the function $u : \Omega \to \mathbb{R}$ was classical solution. Let us take $u_h \in S_h$ which is in general discontinuous in $\mathcal{F}_h$. Combining the terms above with the equation (4.12), we obtain

$$a_h(u_h,\varphi) + J_h(u_h,\varphi) = l_h(\varphi), \tag{4.13}$$

where

$$\begin{aligned} a_h(u,\varphi) = \sum_{K\in\mathcal{T}_h} \int_K u'\varphi'\,\mathrm{d}x - \sum_{x\in\mathcal{F}_h^I} \langle u'\rangle\,[\varphi] - \sum_{x\in\mathcal{F}_h^D} u'\,[\varphi] \\ - \Theta \sum_{x\in\mathcal{F}_h^I} \langle\varphi'\rangle\,[u] - \Theta \sum_{x\in\mathcal{F}_h^D} \varphi'\,[u] \end{aligned}$$

is the *DG diffusion form*,

$$J_h(u,\varphi) = C_W \sum_{x\in\mathcal{F}_h^I} [u]\,[\varphi] + C_W \sum_{x\in\mathcal{F}_h^D} u\varphi$$

is the *interior and boundary penalty form* and

$$l_h(\varphi) = \int_\Omega g\varphi\,\mathrm{d}x + \sum_{x\in\mathcal{F}_h^N} g_N\varphi - \Theta \sum_{x\in\mathcal{F}_h^D} \varphi'\,[u_D] + C_W \sum_{x\in\mathcal{F}_h^D} u_D\varphi$$

is the *right-hand side form.*

Now we can define a *DG finite element solution.*

Definition 17 (DG finite element solution of elliptic problem)**.** *The function $u_h : \Omega \to \mathbb{R}$ is called a DG finite element solution of elliptic problem (4.8)-(4.10) if the following properties hold:*

(i) $u_h \in S_h$.

(ii) The equation (4.13) holds for all $\varphi \in S_h$.

4.4 Implementation

In this section, we discuss the implementation of DG. We ask the question how to define numerical flux at the junctions. In the end, we apply *limiters*.

We use the discontinuous Galerkin method in space and *Adams–Bashforth method* in time. Because we calculate physical quantities (density and velocity), we know that the result must be in some interval. Thus, we use limiters after every iteration to obtain the solution in an admissible interval. In this section, we consider the general hyperbolic problem (4.1)-(4.3).

We use the notation from Section 4.1. We take the partition of space with equidistant interpolation points. For practical purposes, the basis of the test functions space should contain functions from S_h which are non-zero on one element and zero on the other elements. We take these functions such that they are orthogonal to each other in the $L^2(a,b)$ space with the scalar product $(u,v) = \int_a^b uv \,\mathrm{d}x$. Thus, we use *Legendre polynomials*. We know, that $\|p\|^2_{L^2(a_K,b_K)} = h$, where p is a Legendre polynomial and h is the size of one element. The maximal degree of Legendre polynomials is the same as the required degree of the approximate solution. B denotes this orthogonal basis.

To evaluate the integrals over elements, we need numerical integration. We use the *Gauss–Legendre quadrature rule*. If we use n quadrature points (nodes), the Gauss–Legendre quadrature rule is exact for polynomials of degree $2n-1$. We need to keep in mind, that we integrate the product of two functions. If we approximate the solution by a piecewise linear function, we need to integrate polynomials of degree 2. Thus, we need 2 quadrature points.

4.4.1 Time discretization

Let $u_h(x,t) \in \mathbb{R}$ be our solution at the position x at the time t and $B = \{\varphi_1,\ldots,\varphi_N\}$ be the basis of the test functions space, which was described above. We write our solution in the form:

$$u_h(x,t) = \sum_{j=1}^{N} u_j(t)\varphi_j(x),$$

where $u_j(t) \in \mathcal{C}^1(\mathbb{R})$. Due to the linearity of the weak form (4.6) in variable φ, we can use only the elements of basis B instead of all test functions $\varphi \in S_h$. Thus, we can reformulate the property (iv) in Definition 16 as

$$\sum_{j=1}^{N}\left(\frac{\mathrm{d}u_j(t)}{\mathrm{d}t}\,(\varphi_j,\varphi_i)\right) - \sum_{K\in\mathcal{T}_h}\int_K f(u_h)\varphi_i' \,\mathrm{d}x + \sum_{x\in\mathcal{F}_h} H(u^{(L)},u^{(R)})\,[\varphi_i] = (g,\varphi_i) \quad (4.14)$$

for all $\varphi_i \in B$ and for all $t \in (0,T)$. Since the elements of basis B are orthogonal and φ_i is non-zero only on $K_i \in \mathcal{T}_h$, we can write the equation (4.14) as

$$h\,\frac{\mathrm{d}u_i(t)}{\mathrm{d}t} - \int_{K_i} f(u_h)\varphi_i' \,\mathrm{d}x + \sum_{x\in\{a_{K_i},b_{K_i}\}} H(u^{(L)},u^{(R)})\,[\varphi_i] = \int_{K_i} g\varphi_i \,\mathrm{d}x.$$

This leads to a system of N ODEs for unknowns $u_i(t)$, $i = 1,\ldots,N$. Now, we introduce the time discretization.

As we mention above, we discretize the time by the Adams-Bashforth method. This method is a linear multistep method for ODEs. We want to solve our system of ODEs

$$\frac{\mathrm{d}u_j}{\mathrm{d}t} = F_j, \qquad j = 1,\dots,N,$$

where $u_j(t) : \mathbb{R} \to \mathbb{R}$ are unknowns and

$$F_j\left(u_h(t),t\right) := \frac{1}{h}\left(\int_{K_i} g\varphi_i \,\mathrm{d}x + \int_{K_j} f(u_h)\varphi_j' \,\mathrm{d}x - \sum_{x\in\{a_{K_j},b_{K_j}\}} H(u^{(L)},u^{(R)})\left[\varphi_j\right]\right).$$

The right-hand sides F_j are non-linearly depending on the unknowns. We take the time step τ. Then we obtain discrete time values $t_i = i\tau$, where $i \in \mathbb{N}$. We denote $u_j^i := u_j(t_i)$ and $F_j^i := F_j\left(u_h(t_i),t_i\right)$. We use one of the equations in Table 4.1 where S denotes the number of steps. The equations from the table are derived in the lecture notes by Janovský [20]. The first equation is called the forward Euler method. We have u_j^0 from the initial condition. Then we can use the Euler method to calculate the first time step. Thus, we obtain u_j^1. If the Euler method is good enough, we still use this method. Otherwise, we can use the two-steps method and so on.

S	Equation
1	$u_j^{i+1} = u_j^i + \tau F_j^i$
2	$u_j^{i+2} = u_j^{i+1} + \tau\left(\frac{3}{2}F_j^{i+1} - \frac{1}{2}F_j^i\right)$
3	$u_j^{i+3} = u_j^{i+2} + \tau\left(\frac{23}{12}F_j^{i+2} - \frac{4}{3}F_j^{i+1} + \frac{5}{12}F_j^i\right)$
4	$u_j^{i+4} = u_j^{i+3} + \tau\left(\frac{55}{24}F_j^{i+3} - \frac{59}{24}F_j^{i+2} + \frac{37}{24}F_j^{i+1} - \frac{3}{8}F_j^i\right)$
5	$u_j^{i+5} = u_j^{i+4} + \tau\left(\frac{1901}{720}F_j^{i+4} - \frac{1387}{360}F_j^{i+3} + \frac{109}{30}F_j^{i+2} - \frac{637}{360}F_j^{i+1} + \frac{251}{720}F_j^i\right)$

Table 4.1: Adams-Bashforth formulae for different numbers of steps.

4.4.2 Numerical fluxes at junctions

If we would like to model traffic on networks, there arise special problems with numerical fluxes at junctions. We must decide, which values are from the left and which from the right. We use the notation from Section 3.4.

Our aim is to conserve the number of cars at the junctions. The number of cars which inflow or outflow through the junction is given by the traffic flow Q_e. More precisely, the traffic flow from incoming road I_i, $i = 1,\dots,n$, at time t is given by $Q_e\left(\rho_i(b_{i-},t)\right)$. Due to the traffic-distribution matrix, we know the ratio of the traffic flow distribution between the outgoing roads. Thus, the traffic flow to the outgoing road I_j, $j = n+1,\dots,n+m$, at time t is given by $Q_e\left(\rho_j(a_{j+},t)\right) = \sum_{i=1}^n \alpha_{j,i} Q_e\left(\rho_i(b_{i-},t)\right)$. We know that the traffic flow at the boundary of the element is represented by the numerical flux. The DG solution on the i^{th} road is

denoted by ρ_{hi}. Thus, we take the numerical flux $H_j(t)$ at the left point of the outgoing road I_j, i.e. point at the junction, at time t as

$$H_j(t) := \sum_{i=1}^{n} \alpha_{j,i} H(\rho_{hi}(b_{i-},t),\rho_{hj}(a_{j+},t)),$$

where $j = n+1,\dots,n+m$. The numerical flux $H_j(t)$ approximates the traffic flow $Q_e\left(\rho_j(a_{j+},t)\right)$. Similarly, we take the numerical flux $H_i(t)$ at the right point of the incoming road I_i, i.e. point at the junction, at time t as

$$H_i(t) := \sum_{j=n+1}^{n+m} \alpha_{j,i} H(\rho_{hi}(b_{i-},t),\rho_{hj}(a_{j+},t)),$$

where $i = 1,\dots,n$. The numerical flux $H_i(t)$ approximates the traffic flow $Q_e\left(\rho_i(b_{i-},t)\right)$.

It can be shown, that our solution conserves the number of cars at junctions. But it can be also shown, that it does not satisfy property (ii) in Definition 14.

Theorem 4 (Properties of our solution)**.** *Let us use the method described above.*

a) Our solution ρ_{hi}, $i = 1,\dots,n+m$ satisfies the Rankine-Hugoniot condition (3.20).

b) There exists an example such that our solution ρ_{hi}, $i = 1,\dots,n+m$, does not satisfy the property (ii) in Definition 14.

Proof. a) In our case, we want to show

$$\sum_{i=1}^{n} H_i(t) = \sum_{j=n+1}^{n+m} H_j(t).$$

From the definition of H_i and H_j, we immediately obtain

$$\begin{aligned}\sum_{i=1}^{n} H_i(t) &= \sum_{i=1}^{n}\sum_{j=n+1}^{n+m} \alpha_{j,i} H(\rho_{hi}(b_{i-},t),\rho_{hj}(a_{j+},t)) \\ &= \sum_{j=n+1}^{n+m}\sum_{i=1}^{n} \alpha_{j,i} H(\rho_{hi}(b_{i-},t),\rho_{hj}(a_{j+},t)) = \sum_{j=n+1}^{n+m} H_j(t).\end{aligned}$$

b) Let us take the situation with one incoming and two outgoing roads. We want to show that $H_2(\cdot) \neq \alpha_{2,1} H_1(\cdot)$ or $H_3(\cdot) \neq \alpha_{3,1} H_1(\cdot)$. Assume that $\rho_{h1}(b_{1-},0) = 0.5$, $\rho_{h2}(a_{2+},t) = 0.2$, $\rho_{h3}(a_{3+},t) = 0$, $\alpha_{2,1} = 0.75$ and $\alpha_{3,1} = 0.25$. We use the Greenshields model (with $v_{\max} = \rho_{\max} = 1$) and the Lax-Friedrichs flux (4.7). Then

$$H_2(0) = \alpha_{2,1} H(\rho_{h1}(b_{1-},0),\rho_{h2}(a_{2+},0)) = 0.22125$$

and

$$H_1(0) = \alpha_{2,1} H(\rho_{h1}(b_{1-},0),\rho_{h2}(a_{2+},0)) + \alpha_{3,1} H(\rho_{h1}(b_{1-},0),\rho_{h3}(a_{3+},0)) = 0.315.$$

Since $H_2(0) = 0.2212 \neq 0.23625 = \alpha_{2,1} H_1(0)$, we find an example, where the property (ii) in Definition 14 in not satisfied. □

Due to the good results of our model, we would like to interpret the differences between our solution and the admissible traffic solution from Definition 14 and put our solution into the real traffic situation.

The method how to obtain a solution which satisfies the properties from Definition 14 is described in the book [15] or paper [21]. As an example, we take the junction with one incoming and two outgoing roads. For simplicity, we fix the time. We compare the maximum possible fluxes which can inflow into the junction from the incoming road ($\gamma_1^{\max}$) or outflow from the junction to the outgoing roads ($\gamma_2^{\max}$ and $\gamma_3^{\max}$). We take $\gamma = \min\{\gamma_1^{\max}, \frac{\gamma_2^{\max}}{\alpha_{2,1}}, \frac{\gamma_3^{\max}}{\alpha_{3,1}}\}$ and use it as inflow into the junction from the incoming road, i.e. $\widehat{H}_1 = \gamma$. We obtain the outflow through the outgoing roads as an inflow multiplied by the traffic-distribution coefficients, i.e. $\widehat{H}_2 = \alpha_{2,1}\gamma$ and $\widehat{H}_3 = \alpha_{3,1}\gamma$. Thus, if there is a traffic jam in one of the outgoing roads, the cars cannot go into the second outgoing roads, either.

In our model, we calculate the numerical fluxes, where the left value is the traffic density of an incoming road and the right value is the traffic density of one of the outgoing roads. Then we take the possible fluxes and multiply them by the traffic-distribution coefficients. Thus, if there is a traffic jam in one of the outgoing roads, the cars can still go into the second outgoing road according to the traffic-distribution coefficients. So, we model something which corresponds to turning lines. The advantage is that our traffic does not collapse due to the traffic jam on one of the outgoing roads. Since the macroscopic models are aimed for the long (multi-line) roads with huge number of cars, our model makes sense in this situation. The original approach from Definition 14 is aimed for one-line roads, where overtaking is not possible.

In other words, in the model of [15] and [21], a traffic jam on outgoing road blocks the traffic on the incoming road, since cars that want to go to another road cannot overtake the standing cars. In our model this is possible, and the standing cars do not block the incoming road due to overtaking.

The disadvantage of our model is that we do not conserve the traffic-distribution. It could correspond with the real traffic situation where the cars decide to use another road instead of staying in the traffic jam. The problem is when there is no traffic jam. Because we do not control the traffic-distribution, we do not conserve it, see Proof of Theorem 4. This problem will be our aim in the future works, where we would like to present the nonconstant traffic-distribution matrix, which conserve the required traffic-distribution.

4.4.3 Limiters

Our solution could be a physical quantity. Thus, we have some admissibility conditions, e.g. $\rho \in [0,\rho_{\max}]$. If we obtain a solution which is not in the admissible interval, e.g. due to overshoots or undershoots, we must put it in this interval. As an example, we take the traffic density ρ as a solution.

It is important to not change the total number of cars. We introduce a method which works for the linear approximation of the traffic density in LWR models. Assume the space discretization from the beginning of this section. Let K be the element with the described problem, i.e. there exists $x \in [a_K,b_K]$ such that $\rho(x) \notin [\rho_{\min},\rho_{\max}]$.

If the average density on element K is not in the admissible interval $[\rho_{\min},\rho_{\max}]$,

then we change the solution such that $\rho \equiv \rho_{\max}$ or $\rho \equiv \rho_{\min}$ on the whole element K. This operation changes the number of cars, which we do not want. We rather use other changes, e.g. we decrease the time step or increase the number of elements.

If the average density on element K is in admissible interval, we decrease the slope of our solution so that the modified density lies in $[\rho_{\min},\rho_{\max}]$. We can see the process in Figure 4.1. In that example, we have the left side below $\rho_{\min} = 0$. Thus, we make our solution more horizontal. The important property is that the integral $\int_{a_K}^{b_K} \rho(x)\,\mathrm{d}x$ does not change after the application of the limiter.

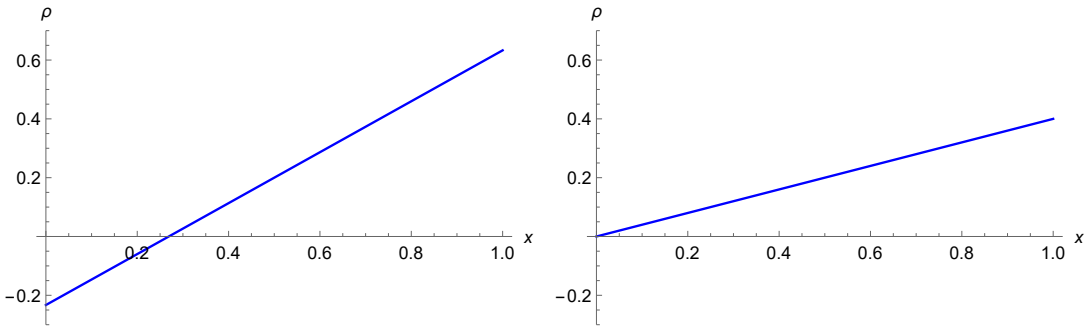

(a) Before applying the limiter.

(b) After applying the limiter.

Figure 4.1: The application of our limiter.

The limiters can provide also the stability of our solution. If the discontinuous Galerkin method has jumps of the solution near discontinuities which are unphysical, we use the limiters to make the solution more "well-behaved". This is good to prevent spurious numerical oscillations. To handle this problem, we follow the paper by Shu [18].

We calculate the solution by one of the methods in Table 4.1. The solution, which we obtain, is considered as a preliminary solution and we denote it $u_h^{i+1,\mathrm{pre}}$. Then, we apply the limiting procedure to go from $u_h^{i+1,\mathrm{pre}} \in S_h$ to $u_h^{i+1} \in S_h$. This procedure should satisfy the following conditions:

- In each element, it does not change the averages of $u_h^{i+1,\mathrm{pre}}$, i.e. the averages of u_h^{i+1} and $u_h^{i+1,\mathrm{pre}}$ are the same in each element. This is for the conservation property of the DG method.

- It does not affect the accuracy of the method in smooth regions, i.e. if $u_h^{i+1,\mathrm{pre}}(x)$ is smooth function for all $x \in M$, $M \subseteq \Omega$, then $u_h^{i+1}(x) = u_h^{i+1,\mathrm{pre}}(x)$ in M.

For simplicity, we omit the upper index $i+1$.

There are many different types of limiters. The problem is still open and there is an active research area. In our program, we use the *modified minmod limiting* from paper [22].

We denote the average of the preliminary solution u_h^{pre} on element $K_i \in \mathcal{T}_h$ as

$$\overline{u}_i = \frac{1}{h}\int_{K_i} u_h^{\mathrm{pre}}\,\mathrm{d}x \tag{4.15}$$

and further denote

$$\tilde{u}_i = u_h^{\mathrm{pre},(L)}(b_{K_i}) - \overline{u}_i, \qquad \tilde{\tilde{u}}_i = \overline{u}_i - u_h^{\mathrm{pre},(R)}(a_{K_i}).$$

As we mention above, the limiter should not change $\overline{u}_i$ but it may change $\tilde{u}_i$ or $\tilde{\tilde{u}}_i$. In particular, minmod limiting changes $\tilde{u}_i$ and $\tilde{\tilde{u}}_i$ into

$$\tilde{u}_i^{\mathrm{mod}} = m\left(\tilde{u}_i,\, \triangle_+\overline{u}_i,\, \triangle_-\overline{u}_i\right), \qquad \tilde{\tilde{u}}_i^{\mathrm{mod}} = m\left(\tilde{\tilde{u}}_i,\, \triangle_+\overline{u}_i,\, \triangle_-\overline{u}_i\right),$$

where

$$\triangle_+\overline{u}_i = \overline{u}_{i+1} - \overline{u}_i, \qquad \triangle_-\overline{u}_i = \overline{u}_i - \overline{u}_{i-1}$$

and the modified minmod function m is defined by

$$m\left(a_1,\, a_2,\, a_3\right) = \begin{cases} a_1, & |a_1| \le Mh^2, \\ \mathrm{sgn}(a_1)\min\left(|a_1|, |a_2|, |a_3|\right), & |a_1| > Mh^2 \text{ and} \\ & \mathrm{sgn}(a_1) = \mathrm{sgn}(a_2) = \mathrm{sgn}(a_3), \\ 0, & \text{otherwise}, \end{cases}$$

where the parameter M must be chosen adequately, see [22]. Then the solution u_h is recovered to conserve the average (4.15) and to satisfy

$$u_h^{(L)}(b_{K_i}) = \overline{u}_i + \tilde{u}_i^{\mathrm{mod}}, \qquad u_h^{(R)}(a_{K_i}) = \overline{u}_i - \tilde{\tilde{u}}_i^{\mathrm{mod}} \tag{4.16}$$

on each element $K_i \in \mathcal{T}_h$. This recovery is unique for P^k polynomials with $k \le 2$. For $k > 2$, we have extra degrees of freedom in obtaining u_h. We could for example choose u_h to be the unique P^2 polynomial satisfying (4.15) and (4.16).

5. Numerical results

In this chapter we present our program and numerical results. Our program is written in the C++ language. It can solve first order hyperbolic problems or second order parabolic problems. Both scalar problems and systems of equations can be solved. As we mention above, we use the combination of Adams-Bashforth method and DG method. We discuss the result of different methods and show the result of calculation on networks. We can compare our results with the approach in the paper [21] where the authors use the *Runge-Kutta method* instead of the Adams–Bashforth method. The Adams–Bashforth is a linear multistep method while the Runge-Kutta is a one-step method.

We calculate the piecewise linear approximations of solutions and we use two quadrature points in each element.

5.1 Comparison of the traffic flow models

We begin with the comparison of the models from Subsection 3.2.1. We use the Greenshields model, Greenberg model and Underwood model. We consider problem (3.12) on a circular road, i.e. we have periodical boundary condition. The length of the road is 1. The initial condition is defined by

$$\rho_0(x) = \begin{cases} 5x - 1.5, & x \in [0.3,0.5], \\ -5x + 3.5, & x \in [0.5,0.7], \\ 0, & \text{otherwise.} \end{cases}$$

Assume that $\rho_{\max} = 1$ and $v_{\max} = 1$. We use the Euler method with the step size $\tau = 10^{-4}$ and the number of elements is $N = 100$. This example is good to study the behaviour of traffic jams.

The first is the Greenshields model. We can see the solution of this model in Figure 5.1 (it is represented by a blue line). We can see the basic phenomenon that the traffic jam moves backward. As the cars leave the traffic jam, the maximal value of traffic density is decreasing, and the traffic jam starts to move forward. We use the limiters for this model and we do not need to be afraid of the case $\rho = 0$.

Our next model is the Greenberg model. Before we start, it is important to note that the equation is not defined for $\rho = 0$ because $V_e(\rho)$ is given by the logarithmic function. Thus, we do not take exactly the value 0 in the initial condition, but we take very small ϵ, e.g. $\epsilon = 10^{-8}$. In this case the limiters are important to prevent the traffic density from reaching the value 0. We can see the solution of this model in Figure 5.1 (it is represented by a red line). In this case the traffic jam moves backward for some time. We can see some differences between this model and the Greenshields model. The density after the traffic jam is not as linear as in the Greenshields model. We can notice that the very low density region disappears. The reason is shown in the fundamental diagram of the Greenberg model (Figure 3.9). The velocity at small density is very high. Thus, the cars at the end of the traffic jam are fast and can reach the traffic jam on the other side of the circular road in a very short time.

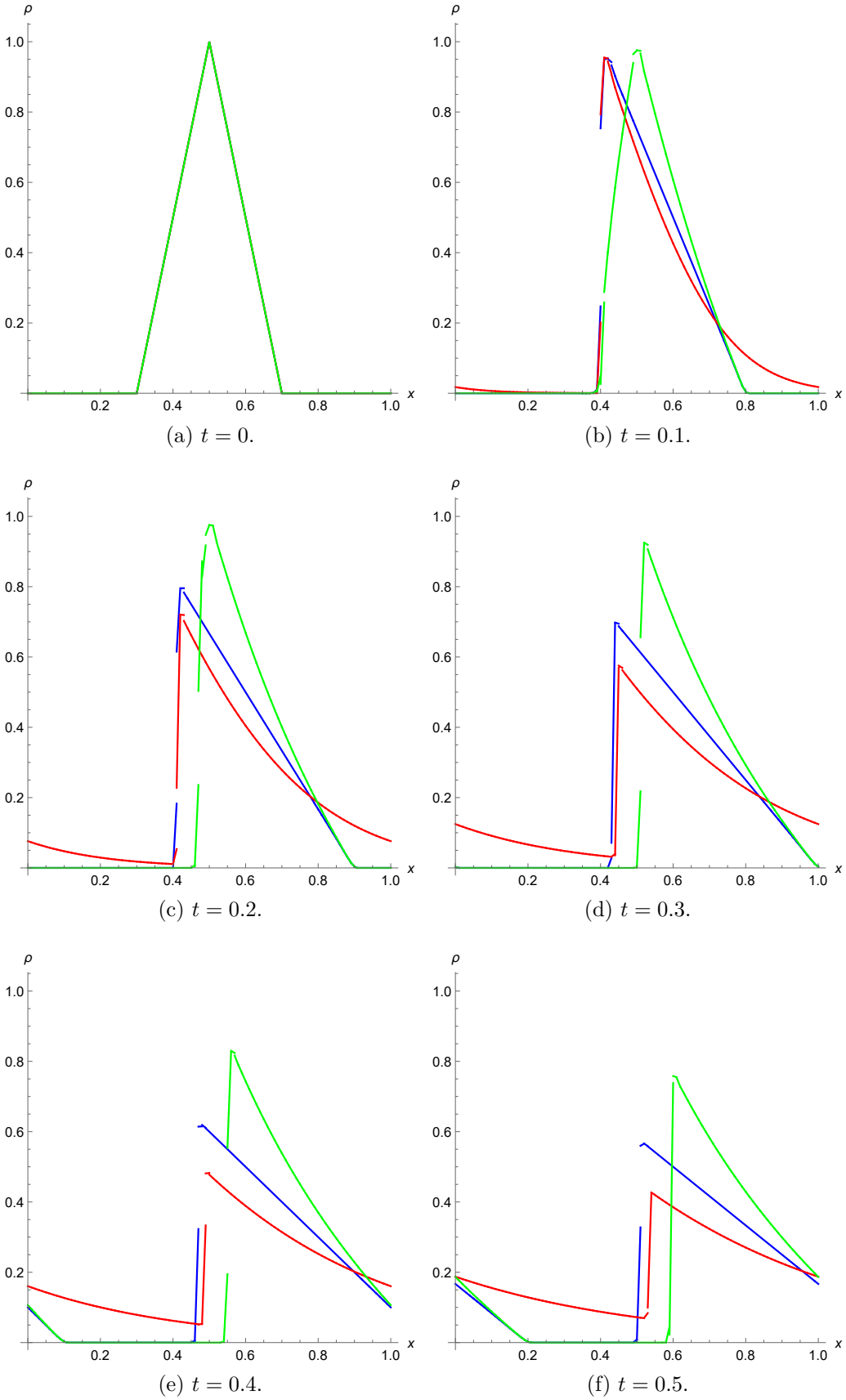

(a) $t = 0$. (b) $t = 0.1$.

(c) $t = 0.2$. (d) $t = 0.3$.

(e) $t = 0.4$. (f) $t = 0.5$.

Figure 5.1: Comparison of the Greenshields, Greenberg and Underwood models.

The last LWR model is the Underwood model. We can see the solution of this model in Figure 5.1 (it is represented by a green line). The main difference is that the traffic jam does not move backward. The reason is shown in the fundamental diagram of the Underwood model (Figure 3.10). The velocity at $\rho_{\max}$ is not 0. Thus, even cars in the traffic jam can move. We use limiters for this model and zero density does not cause problems.

The LWR models converge to the same stationary solution. We can see in Figure 5.2 that the traffic density tends to $\rho \equiv 0.2$ as time t tends to ∞. Thus, we obtain the same results in the closed system independently of the choices of the LWR model. The difference is in how we get to the stationary solution.

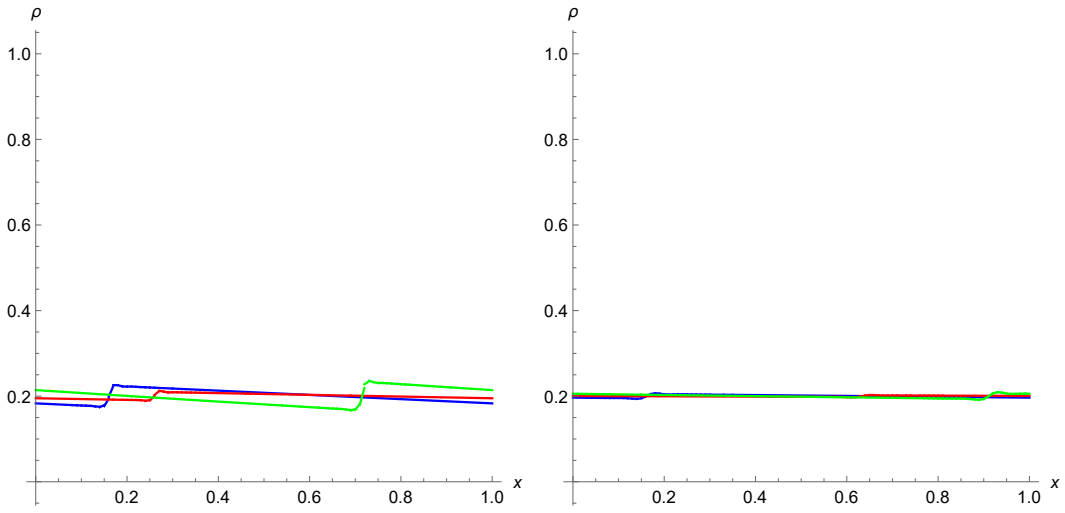

(a) $t = 10$. (b) $t = 50$.

Figure 5.2: Convergence to the stationary solution of the Greenshields, Greenberg and Underwood models.

5.2 Influence of parameters

Now, we compare results from our program to the exact solution. We use the Greenshields model and we have a Riemann problem on a circular road, i.e. we have periodical boundary condition. The length of the road is 1. We want two jumps; one at 0 and second at 0.5. So, we obtain both a rarefaction wave and a shock wave. Assume that $\rho_{\max} = 0.5$ and $v_{\max} = 0.5$. The initial condition is defined by

$$\rho_0(x) = \begin{cases} 0, & x \leq 0.5, \\ 0.5, & x > 0.5. \end{cases}$$

The difference between the approximate solution and exact solution is shown in Figure 5.3. We use the Euler method with the step size $\tau = 10^{-4}$ and the number of elements is $N = 100$. As we can see, we obtain the largest error at $x = 0.5$. Thus, the main problem is caused by the shock wave.

We try different settings of τ, N and the type of multistep method S. We can see the result in Table 5.1. Due to the approximation of the shock wave, the L^∞

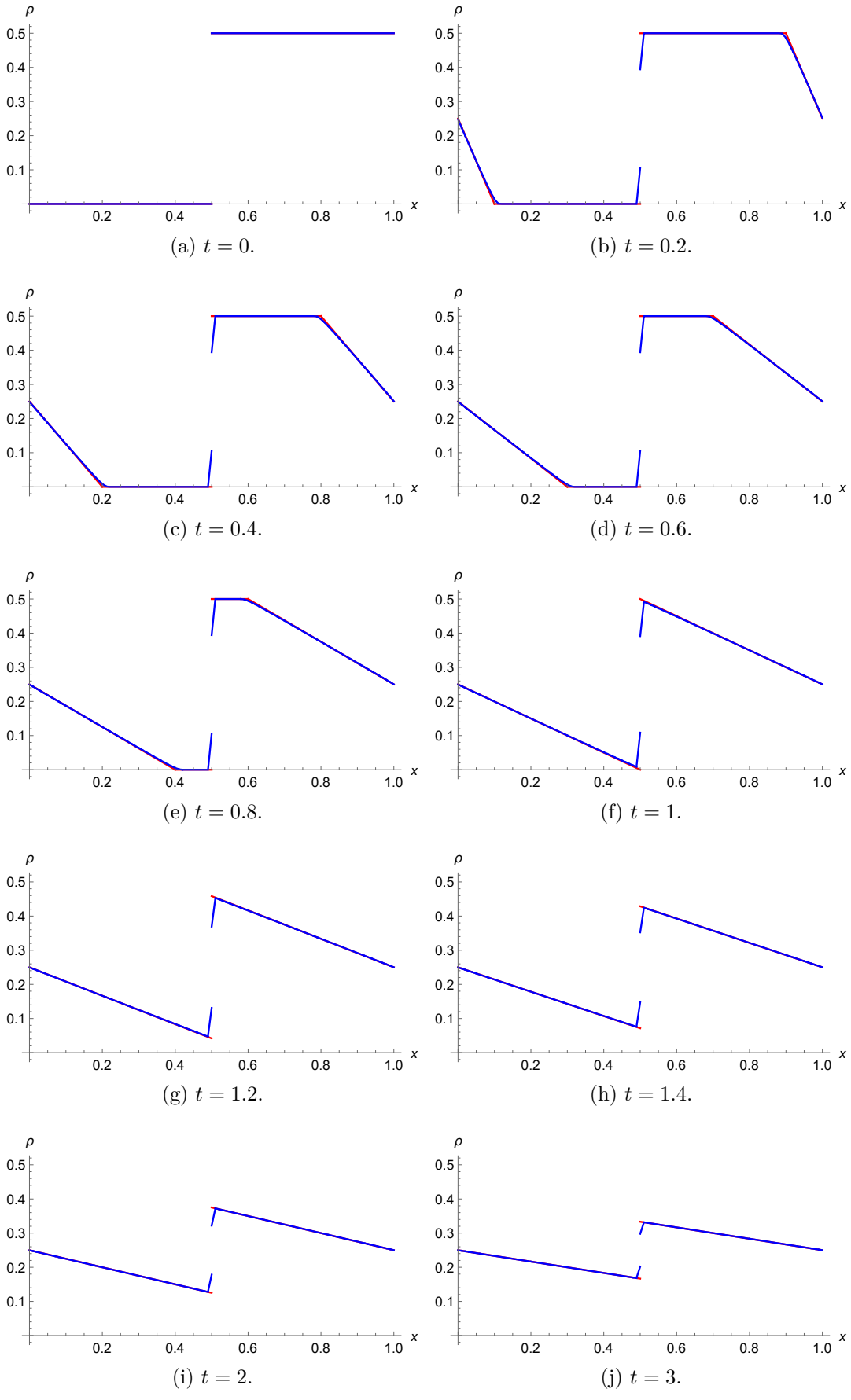

(a) $t = 0$. (b) $t = 0.2$.

(c) $t = 0.4$. (d) $t = 0.6$.

(e) $t = 0.8$. (f) $t = 1$.

(g) $t = 1.2$. (h) $t = 1.4$.

(i) $t = 2$. (j) $t = 3$.

Figure 5.3: Comparison of the approximate and exact solutions.

norm of error is quite large. Next, we can notice that using the Euler method is good enough for this example. Using more steps does not help to reduce the error. Even the changing of step size τ does not help. On the other hand, adding elements is very useful. The L^1 error in the case where $N = 100$, i.e. the length of the element is $h = 0.01$, is approximately twice as large as the L^1 error in the case where $N = 200$, i.e. $h = 0.005$. This is very important to know that the number of elements makes the solution more accurate. Thus, the error is propagated in the space, not in the time.

			$t = 1$		$t = 3$	
S	τ	N	L^1 error	L^∞ error	L^1 error	L^∞ error
1	10^{-4}	100	0.001814	0.086862	0.000453	0.028101
		200	0.000910	0.085212	0.000219	0.027945
	10^{-5}	100	0.001814	0.087018	0.000460	0.028092
		200	0.000913	0.085595	0.000227	0.027935
2	10^{-4}	100	0.001815	0.087035	0.000460	0.028091
		200	0.000914	0.085575	0.000228	0.027934
	10^{-5}	100	0.001815	0.087035	0.000460	0.028091
		200	0.000914	0.085578	0.000228	0.027934
3	10^{-4}	100	0.001815	0.087035	0.000460	0.028091
		200	0.000914	0.085584	0.000228	0.027934
	10^{-5}	100	0.001815	0.087035	0.000460	0.028091
		200	0.000914	0.085578	0.000228	0.027934

Table 5.1: Error of the solution.

Now we demonstrate the difference between the method with and without limiters. The norm of the error is similar in both cases. The difference is in the admissibility of the solution. As we can see in Figure 5.4, the solution with limiters is in the interval $[\rho_{\min},\rho_{\max}]$, where $\rho_{\min} = 0$ and $\rho_{\max} = 0.5$ in our example. When we do not use limiters, our solution is outside the admissible interval. That is the reason why we use limiters.

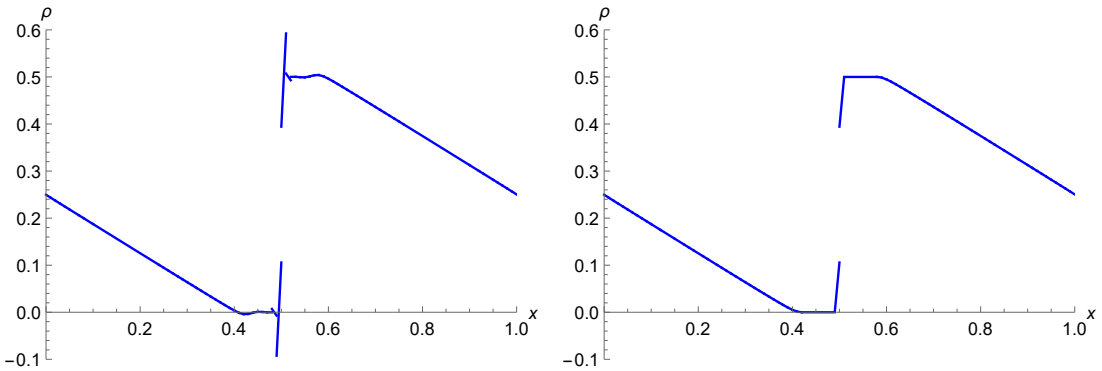

(a) Without limiters.

(b) With limiters.

Figure 5.4: Influence of limiters on the solution. ($t = 0.8$)

5.3 Networks

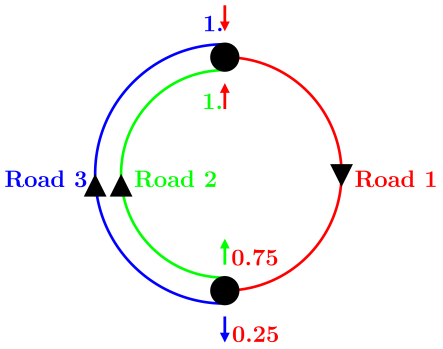

Figure 5.5: Our test network.

We would like to demonstrate how our program computes traffic on networks. Thus, we define network from Figure 5.5. This network is closed, so we can show the conservation of the number of cars. We have three roads and two junctions. The length of all roads is 1. At the first junction we have one incoming road and two outgoing roads. At the second junction we have the opposite situation. We use a different distribution of cars at the first junction. Assume that $\frac{3}{4}$ go from the first road to the second and $\frac{1}{4}$ from the first road to the third. We denote the distribution matrix for the first junction as A_1 and the distribution matrix for the second junction as A_2. Then

$$A_1 = \begin{bmatrix} 0.75 \\ 0.25 \end{bmatrix}, \qquad A_2 = \begin{bmatrix} 1 & 1 \end{bmatrix}.$$

Matrix A_2 does not satisfy the technical condition c) from Subsection 3.4.2. We define different initial conditions for each road. The initial condition for the first road is defined by

$$\rho_0(x) = \begin{cases} 5x - 1.5, & x \in [0.3,0.5], \\ -5x + 3.5, & x \in [0.5,0.7], \\ 0, & \text{otherwise.} \end{cases}$$

The second and third road has a constant initial condition equal to 0.4. The total number of cars in the whole network is 1. We use the Greenshields model on all roads. But we can choose an arbitrary LWR model. We use the Euler method with the step size $\tau = 10^{-4}$ and the number of elements is $N = 100$.

We can see the results in Figure 5.6. Road 1 distributes the traffic density between the other roads. We have too many cars at the second junction, where we have two incoming roads. Thus, we create a traffic jam on Road 2 and Road 3. We can observe the transporting and the distribution of the jump from the first road through the junction on the Figure 5.6g and Figure 5.6h. The result converges to the stationary solution. The traffic density in Figure 5.6i is close to the stationary solution. We check the total amount of cars. For every iteration, the amount of cars is conserved.

Our program can compute traffic on bigger networks and we are not limited by the number of incoming or outgoing roads at junctions. The problem is with the presentation of results. In the future work, we would like to introduce a graphical output.

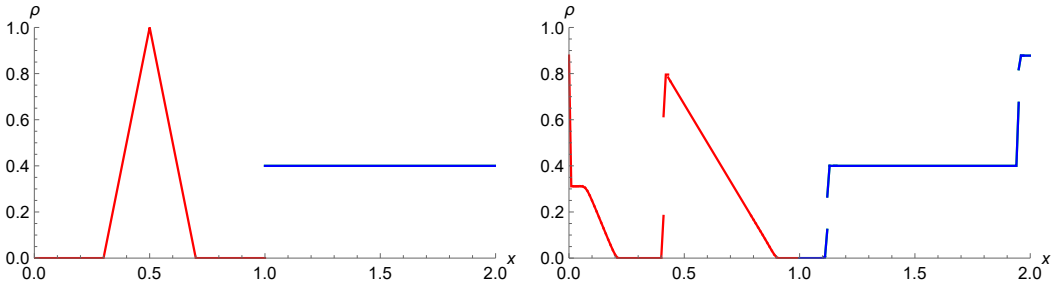

(a) $t = 0$.

(b) $t = 0.2$.

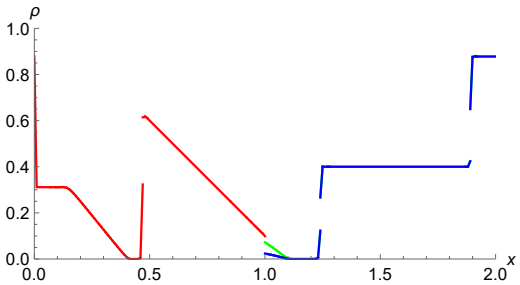

(c) $t = 0.4$.

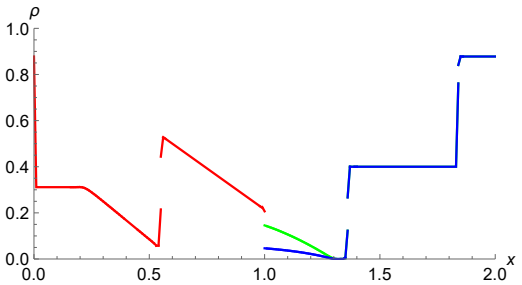

(d) $t = 0.6$.

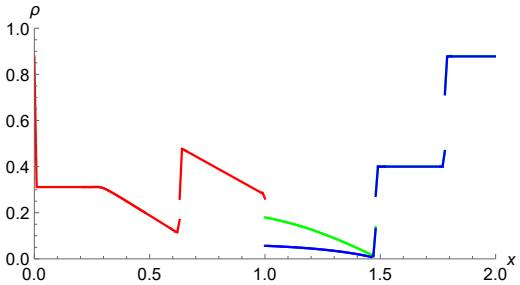

(e) $t = 0.8$.

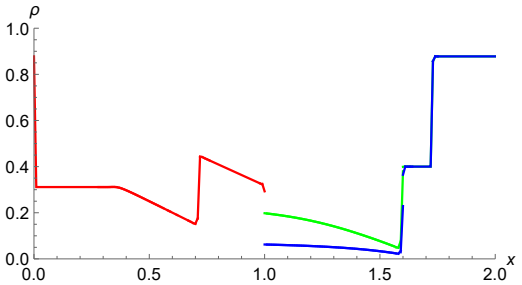

(f) $t = 1$.

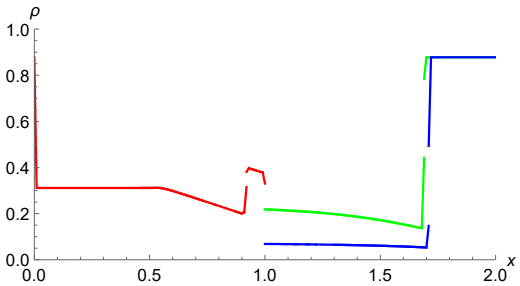

(g) $t = 1.5$.

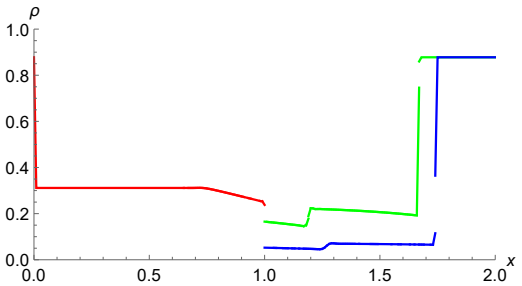

(h) $t = 2$.

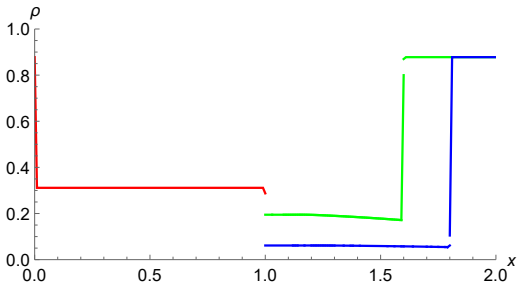

(i) $t = 3$.

Figure 5.6: Network with Road 1, Road 2 and Road 3.

Conclusion

We have presented the basics for the theory of traffic flow for which we showed several approaches. We have explained the difference in microscopic and macroscopic models. Microscopic models simulate every single car. This is very good to imagine the traffic situation. On the other hand, it is very expensive to calculate big systems of ODEs on large networks.

This is the reason why we introduce macroscopic models. Our unknown is the traffic density. Using these models, it is possible to make simulations on big networks with a lot of cars. The disadvantage is that we cannot follow individual cars. We take all the cars as a continuum and study the flow of the traffic. We need to preserve the total amount of cars.

Due to the typical discontinuity of the solution, we use the discontinuous Galerkin method. The discontinuity in the solution is produced by shock waves. For the approximation in time we choose explicit multistep methods. These methods use previous time steps to find the next (future) solution. Thus, we can use the results of previous iteration and the calculation itself is quite fast.

We have created our own program in the language C++. All the methods and models are implemented by us. We had to solve the problem with numerical fluxes at the junctions. The biggest problem was to conserve the number of cars passing through junctions.

The using of DG method on networks is not standard. We were unable to find any work using the same approach as us. We can only compare our approach with the paper [21] by Čanić, Piccoli, Qiu and Ren. They use the discontinuous Galerkin method combined with the Runge-Kutta method.

We use different solutions at the junctions. Our solutions are better on specific types of roads, which are more common for macroscopic models. In the future works, we would like to solve the problem with the conservation of traffic distribution.

As we observed, the use of multistep methods does not bring any major improvements especially in the presence of shock waves. Since the Euler method is good enough in our cases, we do not need to take a higher number of time steps.

This work demonstrated the use of the discontinuous Galerkin method on roads. It is important to have working models which can help us to improve traffic flow. We can model real traffic situations and optimize the timing of traffic lights. The benefits of modelling of traffic flows are ecological and economical. The calculation itself is very fast.

Modelling of traffic flows will have an important role in the future. With a rising number of cars on the roads, we must optimize the traffic situation. That is the reason we started to study traffic flows. We want to continue with this work in the next few years. We would like to improve our program. We are currently looking for interesting projects in traffic modelling.

Bibliography

[1] Femke van Wageningen-Kessels, Hans van Lint, Kees Vuik, and Serge Hoogendoorn. Genealogy of traffic flow models. *EURO Journal on Transportation and Logistics*, 4(4):445–473, 12 2015.

[2] Bruce D. Greenshields. A Study of Traffic Capacity. *Highway Research Board*, 14:448–477, 1935.

[3] R. Eddie Wilson and Jonathan A. Ward. Car-following models: fifty years of linear stability analysis – a mathematical perspective. *Transportation Planning and Technology*, 34(1):3–18, 2011.

[4] Yuki Sugiyama, Minoru Fukui, Macoto Kikuchi, Katsuya Hasebe, Akihiro Nakayama, Katsuhiro Nishinari, Shin-ichi Tadaki, and Satoshi Yukawa. Traffic jams without bottlenecks - experimental evidence for the physical mechanism of the formation of a jam. *New Journal of Physics*, 10, 03 2008.

[5] M. Bando, K. Hasebe, A. Nakayama, A. Shibata, and Y. Sugiyama. Structure stability of congestion in traffic dynamics. *Japan Journal of Industrial and Applied Mathematics*, 11(2):203, 06 1994.

[6] Ingenuin Gasser, Gabriele Sirito, and Bodo Werner. Bifurcation analysis of a class of 'car following' traffic models. *Physica D: Nonlinear Phenomena*, 197(3):222 – 241, 2004.

[7] Kai Nagel and Michael Schreckenberg. A cellular automaton model for freeway traffic. *Journal de physique I*, 2(12):2221–2229, 1992.

[8] Saifallah Benjaafar, Kevin Dooley, and Wibowo Setyawan. *Cellular automata for traffic flow modeling*. Center for Transportation Studies, University of Minnesota, 1997.

[9] Ansgar Jüngel. *Modeling and Numerical Approximation of Traffic Flow Problems*. Universität Mainz, 2002. Available online: `https://www.asc.tuwien.ac.at/~juengel/scripts/trafficflow.pdf`, accessed: 2018-06-29.

[10] Pushkin Kachroo and Shankar Sastry. *Traffic Flow Theory: Mathematical Framework*. University of California Berkeley. In preparation, available online: `https://www.scribd.com/doc/316334815/Traffic-Flow-Theory`, accessed: 2018-04-29.

[11] Olga A. Oleinik. Uniqueness and stability of the generalized solution of the cauchy problem for a quasi-linear equation. *American Mathematical Society Translations*, 2(33):165–170, 1963. English translation.

[12] Lawrence C. Evans. *Partial Differential Equations*. Graduate studies in mathematics. American Mathematical Society, 1998.

[13] Peter D. Lax. *Hyperbolic Systems of Conservation Laws and the Mathematical Theory of Shock Waves*. Number 11–16 in CBMS-NSF Regional Conference Series in Applied Mathematics. Society for Industrial and Applied Mathematics, 1973.

[14] Rainer Ansorge. What does the entropy condition mean in traffic flow theory? *Transportation Research Part B: Methodological*, 24(2):133 – 143, 1990.

[15] Mauro Garavello and Benedetto Piccoli. *Traffic flow on networks*, volume 1. American Institute of Mathematical Sciences (AIMS), Springfield, MO, 2006.

[16] Vít Dolejší, Petr Knobloch, Václav Kučera, and Miloslav Vlasák. *Finite element methods: theory, applications and implementations*. MatfyzPress, Charles University in Prague, 2013.

[17] William H. Reed and T. R. Hill. Triangular mesh methods for the neutron transport equation. Technical report, Los Alamos Scientific Lab., N. Mex.(USA), 1973.

[18] Chi-Wang Shu. Discontinuous galerkin methods: general approach and stability. *Numerical solutions of partial differential equations*, 201, 2009.

[19] Eric Sonnendrücker. *Numerical methods for hyperbolic systems*. Brown University, 2013. Available online: `https://www-m16.ma.tum.de/foswiki/pub/M16/Allgemeines/NumMethHyp/Num-Meth-Hyperbolic-Systems.pdf`, accessed: 2018-04-29.

[20] Vladimír Janovský. *Numerické řešení ODR*. Univerzita Karlova v Praze, 2017. Available online: `https://docs.wixstatic.com/ugd/88996e_ac264b8a8c114e94b2e72771897e96b9.pdf`, accessed: 2018-06-29.

[21] Suncica Čanić, Benedetto Piccoli, Jingmei Qiu, and Tan Ren. Runge-kutta discontinuous galerkin method for traffic flow model on networks. *Journal of Scientific Computing*, 63:31, 03 2014.

[22] Bernardo Cockburn and Chi-Wang Shu. TVB Runge-Kutta Local Projection Discontinuous Galerkin Finite Element Method for Conservation Laws II: General Framework. *Mathematics of Computation*, 52(186):411–435, 1989.

List of Figures

List of Tables